Published in final edited form as:

ACS Biomater Sci Eng. 2021 June 14; 7(6): 2043–2063. doi:10.1021/acsbiomaterials.1c00083.

Methods of Generating Dielectrophoretic Force for Microfluidic Manipulation of Bioparticles

Elyahb A. Kwizera[#a], **Mingrui Sun**[#b], **Alisa M. White**[a], **Jianrong Li**[c], **Xiaoming He**[a,b,d,e,*]

[a]Fischell Department of Bioengineering, University of Maryland, College Park, MD 20742, USA

[b]Department of Biomedical Engineering, The Ohio State University, Columbus, Ohio 43210, USA

[c]Department of Veterinary Biosciences, The Ohio State University, Columbus, OH 43210, USA

[d]Robert E. Fischell Institute for Biomedical Devices, University of Maryland, College Park, MD 20742, USA

[e]Marlene and Stewart Greenebaum Comprehensive Cancer Center, University of Maryland, Baltimore, MD 21201, USA

[#] These authors contributed equally to this work.

Abstract

Manipulation of microscale bioparticles including living cells is of great significance to the broad bioengineering and biotechnology fields. Dielectrophoresis (DEP), which is defined as the interactions between dielectric particles and electric field, is one of the most widely used techniques for the manipulation of bioparticles including cell separation, sorting, and trapping. Bioparticles experience a DEP force if they have a different polarization from the surrounding media in an electric field that is nonuniform in terms of the intensity and/or phase of the electric field. A comprehensive literature survey shows that the DEP-based microfluidic devices for manipulating bioparticles can be categorized according to the methods of creating the nonuniformity via patterned microchannels, electrodes, and media to generate the DEP force. These methods together with the theory of DEP force generation are described in this review, to provide a summary of the methods and materials that have been used to manipulate various bioparticles for various specific biological outcomes. Further developments of DEP-based technologies include identifying materials that better integrate with electrodes than current popular materials (silicone/glass) and improving the performance of DEP manipulation of bioparticles by combining it with other methods of handling bioparticles. Collectively, DEP-based microfluidic manipulation of bioparticles holds great potential for various biomedical applications.

Graphical Abstract

[*]Corresponding author: Mailing address: 8278 Paint Branch Drive, College Park, MD 20742, shawnhe@umd.edu.

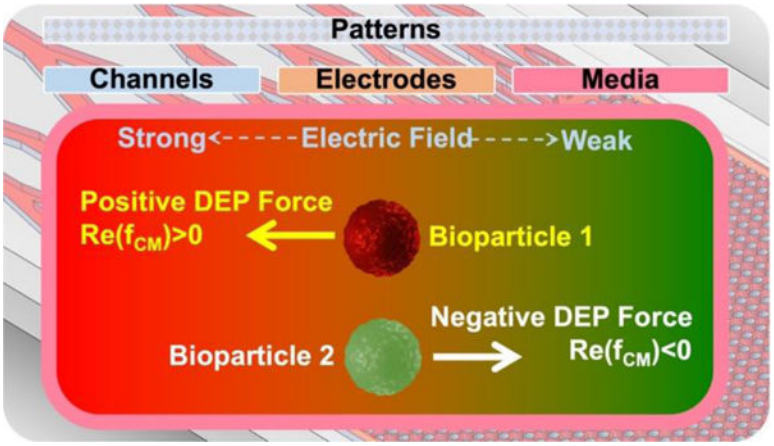

Keywords

Dielectrophoresis; DEP; pattern; cell manipulation; microfluidics; sorting

1. Introduction

Cell sorting/isolation and microfluidics-based cell encapsulation have a wide range of applications in the fields of bioengineering and biotechnology.[1] They are important for stem cell culture and therapy,[2–8] cancer diagnosis,[9–11] drug delivery,[12–14] and water quality analysis.[15–20] Manipulation of microscale bioparticles such as living cells is pivotal to both cell sorting/isolation and microfluidics-based cell encapsulation.[21–46] For instance, in cell sorting/isolation, different types of cells need to be separated based on their geometric, mechanical, electrical, and/or biological properties. Due to its high controllability, convenience, and high efficiency with negligible damages to the cells, microfluidics-based cell manipulation such as cell encapsulation is a valuable technique for 3D cell culture, cell cryopreservation, stem cell therapy, drug delivery, and disease treatment.[47–52] In microfluidics-based cell encapsulation, hydrogel microcapsules are often generated in an oil phase and need to be transferred into an aqueous phase for downstream applications.[53–55]

Various techniques have been used for manipulating microscale bioparticles. Based on the mechanism, bioparticle manipulation can be divided into two categories: extrinsic-property-based manipulation and intrinsic-property-based manipulation.[21] Fluorescence-activated cell sorting,[22–23] magnetic-activated cell sorting,[24–25] and surface-affinity-based separation[26–27] are typical extrinsic-property-based manipulation methods. Dielectrophoresis (DEP) sorting,[56–62] electrophoresis sorting,[28–30] optical sorting,[31] acoustic sorting,[32–34] obstacle-based filtering,[35–38] pinched flow fractionation,[39–40] hydrodynamic filtration,[41] and inertial-lift-force-based separation,[42–46] are typical intrinsic-property-based manipulation methods. Among these methods, DEP has emerged as one of the most widely used techniques for the manipulation of non-living bioparticles. As has been reviewed elsewhere,[63–67] this is possibly because it supports label-free manipulation with high efficiency, biocompatibility, sensitivity, and controllability and allows for highly selective and sensitive analyses due to

its dependence on dielectric properties which constitutes morphological, chemical, and structural characteristics of bioparticles.

However, despite its potential, DEP has not been widely adopted for live cell manipulation, possibly due to many complexities involved with system design. Various factors and variables such as the design of the microfluidic device, fabrication materials, and the medium used for suspending cells, as well as the shape and sizes of the electrodes, and their orientation with respect to the channels play an important role in cell manipulation. Living cells respond differently to electric field gradients due to the differences in their electrical properties. Their responses may also vary based on the electric field strength and frequency, and these properties can be utilized to separate them from other cells. Several recent studies have reported on the dielectrophoretic separation and manipulation of live cells such as white blood cells (WBCs),[68–69] red blood cells (RBCs),[70] cancer cells in suspension,[59, 61] circulating tumor cells (CTCs) in patient blood,[71] and tumor-initiating cells (TICs) or cancer stem cells (CSCs).[57–58, 72] These studies have shown great potential for utilizing DEP in the fields of biotechnology and medicine.

In this review, we summarize the theory of DEP-based microfluidic manipulations of bioparticles with particular emphasis on living cells and classify current DEP devices based on the mechanisms of generating electric field gradient that is a key factor for DEP manipulation. The mechanisms for creating electric field gradients are categorized based on the patterns of channels, electrodes, and media in DEP devices. Moreover, typical devices in each category are illustrated and discussed in an attempt to provide insights into how each of these factors can be adjusted to develop a DEP-based system for efficient bioparticle manipulation.

2. DEP Theory

For bioparticles in a medium under an electric field, there exists electrokinetics, consisting of electroosmosis and electrophoresis which are linearly proportional to the electric field intensity.[73] If the electric field is not homogeneous, there exists DEP-induced motion that has a nonlinear relationship with the electric field intensity.[74] Therefore, any kind of particles in a DEP medium can be manipulated with the use of an electric field.[75–76] The electric field can also be easily controlled by changing certain electric field parameters such as the frequency, magnitude, phase, wave symmetry, and wave shape.[75, 77] In the presence of a small electric double layer and with the Boltzmann distribution, the behavior of bioparticles in a medium under an electric field is governed by the following equations:[73–74]

$$\boldsymbol{J} = -D\boldsymbol{\nabla}c + c(\boldsymbol{u} + \boldsymbol{u}_{EK} + \boldsymbol{u}_{DEP}) \tag{1}$$

$$\boldsymbol{u}_{EK} = \boldsymbol{u}_{EO} + \boldsymbol{u}_{EP} \tag{2}$$

$$\boldsymbol{u}_{EK} = \mu_{EK}\boldsymbol{E} \tag{3}$$

$$\boldsymbol{u}_{EO} = \mu_{EO}\boldsymbol{E} = -\frac{\varepsilon_m \zeta}{\eta}\boldsymbol{E} \tag{4}$$

$$\boldsymbol{u}_{EP} = \mu_{EP}\boldsymbol{E} = \frac{\varepsilon_m \zeta_p}{\eta}\boldsymbol{E} \tag{5}$$

$$\boldsymbol{u}_{DEP} = \mu_{DEP}\boldsymbol{\nabla}|\boldsymbol{E}|^2 \tag{6}$$

where J is the flux of the particles, D is diffusivity, and c is the concentration of bioparticles; $\boldsymbol{u}$, $\boldsymbol{u}_{EK}$, $\boldsymbol{u}_{DEP}$, $\boldsymbol{u}_{EO}$, and $\boldsymbol{u}_{EP}$ are non-electrokinetic, electrokinetic, DEP, electroosmotic, and electrophoretic velocity fields, respectively; μ_{EK}, μ_{EO}, μ_{EP}, and μ_{DEP} are electrokinetic, electroosmotic, electrophoretic, and DEP mobilities, respectively; ε_m is the complex permittivity of the medium, $\boldsymbol{E}$ is the applied electric field, ζ and ζ_p are the zeta potentials at the channel and at the particle surfaces, respectively and η is the fluid viscosity.

2.1. DEP force

A polarizable particle in a medium may experience a DEP force in a non-uniform electric field if the particle has different electric properties from the surrounding medium. There are two kinds of DEP responses:[78–82] positive (pDEP) and negative (nDEP) (Fig. 1a). The former occurs if the polarization of the particle is stronger than that of the medium, which drives the bioparticle to move from a lower electric field intensity region to a higher electric field intensity region. The nDEP response occurs if the polarization of the particle is weaker than that of the medium, which drives the bioparticles to move from high electric field intensity region to a lower electric field intensity region.

Electric fields for DEP can be created using either alternating current (AC) or direct current (DC), to generate different electric field properties for different purposes. The time-dependent force $\boldsymbol{F}(t)$ acting on a polarized particle in a medium with an AC electric field can be calculated as follows:[83]

$$\langle \boldsymbol{F}(t) \rangle = 2\pi\varepsilon_m r^3 \left[Re(f_{CM})\boldsymbol{\nabla} {E_{RMS}}^2 + Im(f_{CM})\left(E_{x0}^2 \boldsymbol{\nabla}\varphi_x + E_{y0}^2 \boldsymbol{\nabla}\varphi_y + E_{z0}^2 \boldsymbol{\nabla}\varphi_z \right) \right] \tag{7}$$

$$\boldsymbol{E}(t) = E_x(t)\hat{\boldsymbol{x}} + E_y(t)\hat{\boldsymbol{y}} + E_z(t)\hat{\boldsymbol{z}} \tag{8}$$

$$E_x(t) = E_{x0} e^{j(\omega t + \varphi_x)} \tag{9}$$

$$E_y(t) = E_{y0} e^{j(\omega t + \varphi_y)} \tag{10}$$

$$E_z(t) = E_{z0} e^{j(\omega t + \varphi_z)} \tag{11}$$

where the $\langle \boldsymbol{F}(t) \rangle$ is time-averaged force, ε_m is the permittivity of the medium, r is the bioparticle radius; f_{CM} is the Clausius-Mossotti (CM) factor; $Re(f_{CM})$ is the real (in-phase) part of the factor f_{CM}, which determines pDEP versus nDEP (Fig. 1a); $Im(f_{CM})$ refers to the imaginary part of the factor f_{CM}; E_{RMS} is the root mean square (RMS) value of the time-averaged electric field; $\boldsymbol{\nabla}$ is the gradient operator; $\hat{\boldsymbol{x}}$, $\hat{\boldsymbol{y}}$, and $\hat{\boldsymbol{z}}$ are unit vectors in the Cartesian coordinate system; $E_x(t)$, $E_y(t)$ and $E_z(t)$ are the electric field components in x, y, and z directions, respectively; E_{x0}, E_{y0}, and E_{z0} are the magnitudes and φ_x, φ_y, and φ_z are the phase angles in x, y, and z directions, respectively; ω is the angular frequency of the applied electric field; and j and t refer to the imaginary symbol and time, respectively. Generally, the CM factor in an AC electric field is defined as follows:[83–84]

$$f_{CM,AC} = \frac{\varepsilon_p^* - \varepsilon_m^*}{\varepsilon_p^* + 2\varepsilon_m^*} \tag{12}$$

where ε_p^* and ε_m^* are the complex permittivities of the bioparticle and the medium, respectively, which can be calculated as follows:[85]

$$\varepsilon_m^* = \varepsilon_m - \frac{j\sigma_m}{\omega} \tag{13}$$

$$\varepsilon_p^* = \varepsilon_p - \frac{j\sigma_p}{\omega} \tag{14}$$

where $j = \sqrt{-1}$, ε_p is the permittivity of the bioparticle, and σ_m and σ_p are the conductivities of the medium and the bioparticle, respectively. If ω becomes zero, it turns into a direct current (DC) electric field for which the conductivity dominates the CM factor. Therefore, the CM factor in a DC electric field can be given as follows:[86–87]

$$f_{CM,DC} = \frac{\sigma_p - \sigma_m}{\sigma_p + 2\sigma_m} \tag{15}$$

Different factors such as local gradient, deformability of a particle's shape, size, and permittivity contribute to the dielectrophoretic velocity.[88] For example, King et al. used a nonuniform AC electric field imposed by planar electrodes patterned on an insulating substrate and coated with a thin dielectric layer, to separate different particles in the submicron range suspended in a liquid.[89] They concluded that the size-based separation occurred due to the positive DEP force imposed by the nonuniform electric field within the liquid. This electric field attracts the larger particles more strongly, leaving the smaller particles to be swept further along in the shear flow. Dielectrophoresis has also been used to separate living cells based on different physical properties such as density and dielectric properties.[68, 90] Yang et al. used dielectrophoretic field-flow-fractionation, a cell-separation technique that exploits the differences in the density and dielectric properties of cells, to separate four major leukocyte subtypes, namely, T- and B-lymphocytes, monocytes, and granulocytes, achieving a purity of more than 90% and a high separation performance.[68] The

cells with different densities and dielectric properties are levitated to different heights inside a thin chamber where they are carried with the fluid-flow and separated by their different velocity profile. Cell sorting occurs due to this difference in velocity, and different cells are collected at varying locations in the chip.

In some DEP devices, both DC and AC electric fields are applied. Typically, the DC electric field is applied on the whole channel to generate an electroosmotic and/or an electrophoretic flow to drive bioparticles to pass through the channel. The electrophoretic motion of particles has been used for many years especially for measuring surface potential.[75] The DC component of DEP force can be calculated as follows:

$$\boldsymbol{F}_{DEP} = 2\left(\alpha^2 + 1\right)\pi\varepsilon_m r^3 Re\left(\frac{\varepsilon_p^* - \varepsilon_m^*}{\varepsilon_p^* + 2\varepsilon_m^*}\right)\boldsymbol{\nabla}|\boldsymbol{E}_{DC}|^2 \tag{16}$$

$$\alpha = \frac{|\boldsymbol{E}_{AC}|}{|\boldsymbol{E}_{DC}|} \tag{17}$$

where $\boldsymbol{E}_{AC}$ and $\boldsymbol{E}_{DC}$ are the intensities of the AC and DC electric field, respectively. Under DC electric field conditions, the existence of electrophoretic movement may cause some undesired negative effects such as the Faradaic reactions at the electrode-electrolyte interface, which can potentially lead to electrode degradation, generation of bubbles in the channels, hydrodynamic instability, and sample contamination. These undesirable problems can be reduced with AC electric fields.[91–93] It is important to note that Eq. (16) is derived by assuming homogeneous spherical bioparticles (Fig. 1b), and it can be modified for non-spherical bioparticles such as ellipsoids, cylindrical rod-shaped, or spheroids.[94–96] However, living cells are not homogeneous and multi-layered models are needed for predicting their DEP forces.

2.2. Single-layer model

The single-layer model assumes that cells are homogeneous dielectric spheres (with radius r, permittivity ε_p^*, and conductivity σ_p^*) that are immersed in the medium with permittivity ε_m^* and conductivity σ_m^* (Fig. 1b).[66] This model has been used to study various cells (Table 1) including blood cells, viruses, eukaryotic single-celled microorganisms (e.g., yeast and algae), and bacterial cells (e.g., Staphylococcus aureus and Mycobacterium smegmatis).[70, 97–102] The magnitude of the time-averaged $\boldsymbol{F}_{DEP}$ exerted on a on a single-layered bioparticle in conventional dielectrophoresis by an AC voltage[97, 103] can be described from eq. (7) as:

$$\boldsymbol{F}_{DEP} = 2\pi r^3 \varepsilon_m Re\left(\frac{\varepsilon_p^* - \varepsilon_m^*}{\varepsilon_p^* + 2\varepsilon_m^*}\right)\boldsymbol{\nabla}|\boldsymbol{E}_{AC}|^2 \tag{18}$$

where ε_p^* is calculated from eq. (14) by taking into account the membrane of the cell and other molecular components that affect the polarization between the cytoplasm and the membrane such as lipid composition and proteins.[104–106]

Su et al. utilized a single layer model to measure electrical properties of cell populations on a cell-by-cell basis by predicting the real part of the Clausius–Mossotti factor to determine the distribution where part of the human Leukemia cell population would experience the positive DEP.[107] They then used this method to find suitable conditions at different frequencies and media conductivities to separate certain cells from their subpopulations. Moreover, with the current exponential rise in the use of cell-derived EVs (i.e. exosome, microvesicles) for disease detection and therapy, DEP has shown excellent potential for rapid isolation and detection of EVs due to its ability to cause minimal damage and significantly reduce processing time while offering high isolation efficiency.[108] Therefore, the single layer model is especially important for determining both the conductivity and the force to be exerted on EVs that are under the electric current at various frequencies. Frusawa et al. used this model to measure the attractive forces acting on leukemia cells, red blood cells, and vesicles that are under AC-DEP in different electrolytes and at different frequencies of sinusoidal electric fields.[109] The obtained magnitude of DEP force was used to better capture vesicles on the electrode needle of a frequency-modulated wave DEP device. The sorting of micro/nanovesicles is of utmost importance for biomolecule characterization and single layer modeling is very critical for evaluating the efficacy and advantages of the proposed DEP sorting methods.

2.3. Multilayer models for living cells

In the two-layer model for living cells (Fig. 1c), the inner layer (or core) is for both the nucleus and cytoplasm while the outer layer is for the membrane.[97, 110–112] According to the DEP theory, the effective complex permittivity can be calculated as follows:[97, 113]

$$\varepsilon_p^* = \varepsilon_{cell}^{eff*} = -\varepsilon_{mem}^* \frac{2(\varepsilon_{n-c}^* - \varepsilon_{mem}^*)r_{n-c}^3 + (\varepsilon_{n-c}^* + 2\varepsilon_{mem}^*)r_{mem}^3}{(\varepsilon_{n-c}^* - \varepsilon_{mem}^*)r_{n-c}^3 - (\varepsilon_{n-c}^* + 2\varepsilon_{mem}^*)r_{mem}^3} \quad (19)$$

where r_{mem} is the radius of the membrane, and ε_{n-c}^* and r_{n-c} are the complex permittivity and the radius of the nucleus and cytoplasm, respectively. r_n and $r_c (= r_{n-c})$ are the radii of the nucleus and cytoplasm, and ε_n^* and ε_c^* are the complex permittivities of the nucleus and cytoplasm, respectively. Additionally, a living cell can be described using a three-layer model (Fig. 1d), where the first layer is the membrane, the second layer is the cytoplasm, and the third layer is the nucleus.[110, 114] Thus, the overall effective complex can be calculated from eq. (19) where ε_{n-c}^* is given by:

$$\varepsilon_{n-c}^* = -\varepsilon_c^* \frac{2(\varepsilon_n^* - \varepsilon_c^*)r_n{}^3 + (\varepsilon_n^* + 2\varepsilon_c^*)r_c{}^3}{(\varepsilon_n^* - \varepsilon_c^*)r_n{}^3 - (\varepsilon_n^* + 2\varepsilon_c^*)r_c{}^3} \quad (20)$$

Furthermore, a cell with a cell wall (e.g., a plant cell) can be modeled using a three-layer model (Fig. 1e), for which the first, second, and third layers are the cell wall, cell membrane, and the cell nucleus and cytoplasm.[65, 102, 115–116] The effective complex permittivity of the cell can be written as follows:[97, 110, 113]

$$\varepsilon_p^* = \varepsilon_{cell}^{eff*} = -\varepsilon_w^* \frac{2(\varepsilon_{n-c-mem}^* - \varepsilon_w^*)r_{n-c-mem}^3 + (\varepsilon_{n-c-mem}^* + 2\varepsilon_w^*)r_w^3}{(\varepsilon_{n-c-mem}^* - \varepsilon_w^*)r_{n-c-mem}^3 - (\varepsilon_{n-c-mem}^* + 2\varepsilon_w^*)r_w^3} \quad (21)$$

$$\varepsilon_{n-c-mem}^* = -\varepsilon_{mem}^* \frac{2(\varepsilon_{n-c}^* - \varepsilon_{mem}^*)r_{n-c}^3 + (\varepsilon_{n-c}^* + 2\varepsilon_{mem}^*)r_{mem}^3}{(\varepsilon_{n-c}^* - \varepsilon_{mem}^*)r_{n-c}^3 - (\varepsilon_{n-c}^* + 2\varepsilon_{mem}^*)r_{mem}^3} \quad (22)$$

where $r_{mem} = (r_{n-c-mem})$, ε_w^* and r_w are the complex permittivity and the radius of the cell wall, respectively.

3. Categories of Microfluidic DEP Devices

A microfluidic DEP device includes microchannels, electrodes, and DEP media. Typically, one aqueous medium, such as an electrolyte solution or a sugar solution, with homogeneous and constant electric properties is used DEP microfluidic device, as summarized in Table 2. As shown in the aforementioned model, an electric field gradient is needed for generating DEP forces on particles. A careful examination of the literature informs us that this has been achieved by creating patterned microchannels, patterned electrodes, and/or patterned DEP media (Fig. 2).

3.1. Patterned microchannels

DEP microfluidic devices that generate electrical field gradient with patterned microchannels can be further divided into contact and contactless DEP based on the presence and absence of direct sample-electrode contact, respectively (Fig. 2).

3.1.1 Contact DEP—An electric field gradient can be generated by insulating obstacles patterned in the main channel. Typically, DEP devices with patterned channels are fabricated using a single material, such as polydimethylsiloxane (PDMS), and the fabrication is simple and low-cost. The masters for the channels are usually created using photolithography. The electrodes are often located far away from the active part of the channels, to reduce the effect of bubble formation and electrode fouling.[117]

Lapizco-Encinas et al. fabricated square, triangular, and circular insulating posts to generate an electric field gradient in a DEP microfluidic device for separating and concentrating live and dead bacterial cells (Fig. 3a).[87, 118–119] The insulating microstructures in the device produced a non-uniform electric field that removed and concentrated bacterial cells in water by dielectrophoretically trapping them upon exertion of the electric field. This insulator-based DEP device showed further potential for applications in different areas such as water purification and protein manipulations. Even though this is the first known DC-insulating DEP (iDEP) device used for live bacteria separation, it has since been applied in the separation of other different cells such as white blood cells,[120] red blood cells,[121] and E.coli bacteria.[122]

Nonuniform electric fields in the patterned channels can be produced by intercalating oil droplets inside the microchannel where the size of the oil droplet can be controlled and

manipulated to achieve certain dynamic insulator-based DEP. Barbulovic-Nad et al. used an oil droplet as the obstacle to control the electric field gradient in a DEP device for sorting polystyrene particles based on their size (Fig. 3b).[123] The separation of the microparticles takes place in a compressed DC field between the channel wall and an oil droplet, and the field gradient leads to the particle separation. Since the separation took place at both lower and higher voltages, this system can be potentially applied to sorting live biological cells and other biological samples that are sensitive to higher electric field intensity. Additionally, insulating blocks inside the microchannel can facilitate the DEP-based bioparticle separation by exerting the negative DEP on bioparticles, forcing them to deviate from their electrokinetic path based on their sizes. Kang et al. reported DEP sorting of different cells based on size using a rectangular or a triangular block (Fig. 3c).[120] With an insulating block inside the microchannel, a mixture of microparticles of different sizes mimicking white and red blood cells were continuously separated into two reservoirs by adjusting the applied voltages at the end of different branches. This separation method offers a high sensitivity at which bioparticles of few to tens of micrometers difference in diameter can be continuously and successfully separated.

The use of embedded electrodes in traditional DEP can lead to fouling and the potential for other electrochemical reactions such as electrolysis, which might alter the sample quality and can be toxic to living cells. To prevent issues associated with traditional electrode-based DEP and iDEP, Srivastava et al. reported a direct current insulator-based DEP device to distinguish the ABO-Rh human blood types based on their erythrocyte antigen expression.[124] They utilized embedded insulating obstacles of different geometries to create a spatial non-uniform DC electric field that is applied remotely, which prevents electrochemical reactions. They were able to determine that the red blood cell polarizability in the electric field depends solely on their membrane antigen expression.

Liquid metal electrodes have also been used to overcome the problems associated with traditional embedded electrodes such as Joule heating and fouling.[125–126] Sun et al. developed a DEP device with liquid electrodes to separate live and dead PC-3 human prostate cancer cells with ~90% separation efficiency and achieved ~95% separation efficiency for PC-3 separating human prostate cancer cell from polystyrene microbeads.[127] The device electrodes were made from an ionic liquid which was immiscible with a cell-suspending DEP medium. The medium was made of a mixture of glucose, sucrose, and PBS. Dynamically, a stable interface between the ionic liquid and the DEP medium was established where an electric field gradient in both electrodes was generated by the conductivity gradient which was used to separate different cells in the main channel.

Of note, the electric field in DEP devices can also be localized to separate a mixture of cells of different origins into distinct populations due to unique responses when cells are under electric field gradient. Kikkeri et al. created and incorporated a passivated-electrode insulator-based DEP microchip to fabricate a separation channel that would expose cells to the DEP forces as they travel through the microchip (Fig. 3d).[128] By incorporating multiple winding rows with several nonuniform structures into the sidewalls of the microchip, they were able to produce a high electric field gradient and a high locally generated DEP force for safely separating cancer cells spiked in whole blood based on their morphology with

90% separation efficiency. The iDEP electrodes can also be externally placed in the inlets and outlets. This not only simplifies the device operations, but also prevents unnecessary fouling, bubble generation, and other electrochemical reactions that are frequently observed in devices where electrodes are embedded inside the channels. Mohammadi et al. designed and manufactured a straight channel based-microfluidic device with dead-end branches on both sides (Fig. 3e).[129] The device uses a low voltage to avoid cell lysis and takes advantage of hydrodynamic effects to capture RBCs in the dead-end branches before the field gradient is applied. Once the electric field is applied, the electro-osmotic flow is generated to remove the RBCs from the central part of the channel, effectively making an RBC-free zone of plasma with a 99% purity.

By adding a longitudinal feature to insulator based dielectrophoresis to generate a gradient of dielectrophoretic traps in a microchannel with a patterned structure, Pysher et al. developed a sawtooth geometry based-DEP device to separate live bacterial cells in the weaker DEP traps and dead bacterial cells in the stronger DEP traps (Fig. 3f).[86] When the field was applied, the device continuously resolved the separation of the bacterial cells according to both their electrophoretic and dielectrophoretic characteristics. This technique is very versatile for biological cell sorting, although further studies are warranted to achieve precise control over the resolution. Jones et al. modified the aforementioned sawtooth device by changing the tooth insulator geometry to create distinct zones of increasing local electric field gradient along the length of the channel.[122] When three serotypes or strains of Escherichia coli bacteria are driven through the channel, they encounter zones of increasing DEP force as they approach each set of opposing teeth and are separated based on their characteristic electrokinetic properties. With this device, red blood cells were successfully and reproducibly isolated from whole blood (Fig. 3g).[121] It is worth noting that the geometry of the converging channel (e.g., the sawtooth microchannel) provides an important advantage of allowing for controlled variation of electric field gradient that leads to the increased strength of the DEP force acting on the particle. However, recent numerical simulation studies[130–134] that have been experimentally confirmed,[135–136] have shown that, due to a DC electrokinetic flow which gives rise to negative DEP force in converging/diverging microchannel, particles can experience a chocking phenomenon. During this process, DEP force can surpass other effects such as electrophoresis and electro-osmosis,[131] which prevents the particles from moving further into the converging channel. Even though this phenomenon can be disadvantageous for some studies like particle separation[137] or particle focusing,[135] it is important for some applications including bioparticle trapping,[138–139] cell sorting,[86, 140] and some concentration procedures.[118]

Importantly, patterned microchannels can be angled to constrict the depth of the channel. This provides some additional degrees of freedom by which the bioparticles in the system are governed by the magnitude of the DEP force. Hawkins et al. reported an insulative DEP device with an angled structure to separate polystyrene spheres of different sizes to mimic Mycobacterium cells (Fig. 3h).[74] The device uses DEP effects to transverse channel position and DC-offset-DC electric fields to control the electrokinetic effect on the bioparticles. It overcomes the limitations brought by traditional insulation-based DEP by decoupling linear and nonlinear electrokinetic effects and actuating nonlinear forces.

One of the main hurdles in traditional cell sorting techniques is the lack of separation of different cells of different origins. By modifying AC electrical frequency changes in different media of varying conductivities, DEP response from cells of varying origin can be measured by leveraging the difference in crossover frequency for each cell type to determine an appropriate frequency at which the cells of different origins can be separated. Alshareef et al. demonstrated the use of a dielectrophoretic lab-on-a-chip device that can effectively separate different cancer cells of different epithelial origin by adjusting the frequency in diluted phosphate-buffered saline (PBS, Fig. 3i).[141] With this device, MCF-7 breast cancer cells, and HCT-116 colorectal cancer cells were efficiently separated from each other by finding a frequency at which one cell type experienced a negative DEP, while the other cell experienced no DEP force. Another bottleneck of conventional cell sorting techniques is the inability to separate the flow and capture zones which leads to lower capture efficiency and cell damages caused by higher flow speeds. To address this issue, Sun et al. created a patterned DEP-based microfluidic device, ZonesChip, with separate capture and flow zones created to isolate circulating tumor cells (CTCs) from blood (Fig. 4a).[71] Two copper wires were inserted into the two sides of the main channel. When the electric field was applied, an electric field gradient was generated by patterned PDMS microposts. The main channel is separated into a flow zone (with high flow speed and low electric field intensity) and a capture zone (with low flow speed and high electric field intensity). DEP force drives the cells from the flow zone into the capture zone (Fig. 4b), which contributes to the high throughput and high efficiency for CTC detection using the device.

3.1.2 Contactless DEP—In contactless DEP devices, thin insulating barriers are fabricated between electrodes and the main microchannel. Therefore, the non-uniform electric field in the main channels that is necessary for DEP cell manipulation can be achieved without any direct contact of the electrodes with the sample. The contactless DEP devices also rely on patterned structures in the main channel to generate an electric field gradient, meaning the gradient is generated by the geometry of the insulating structures in the main channel.[142] Liquid electrodes (e.g., salt solutions) are typically used in contactless DEP devices, where the conductivity of the liquid electrodes is much higher than that of the samples. The insulating barriers also act as a capacitor to couple the electrodes and the main microchannel; therefore, the electric field gradient can be generated in the main channel by applying an AC field across the barrier. Typically, the frequency of the electric field applied on the device is high in order to overcome the thin insulation barrier between the electrode and sample, so that a sufficient electric field intensity is generated in the main microchannel for manipulating bioparticles. Similar to contact DEP devices, contactless DEP devices are low-cost and can be fabricated easily. Additionally, the thin insulating barriers between electrodes and samples in the contactless DEP devices can prevent bubble formation and electrode fouling. However, in order to cross the insulating barrier and generate a strong electric field gradient, contactless DEP devices require a very high voltage with high frequency.[127] In some DEP devices, only a positive DEP response can be applied, because the breakdown voltage of the thin barrier limits the use of negative DEP response. Shafiee et al. reported the concept of contactless DEP (Fig. 5a) and found that cells present unique DEP responses in the contactless DEP device, which demonstrates the potential applications of this device for cell sorting.[142] In this device, the electric field was created in the sample

microchannel using electrodes that are not in direct contact with the biological sample. The electrodes are, instead, directly inserted into microchambers and are separated from the sample by thin insulators. Using this device, they were able to identify various cells from three different cell lines based on their electrical properties without contamination from electrodes. Liquid electrodes-based devices are advantageous because they do not require metal electrodes and do not need to be bonded to PDMS. Shafiee et al. developed a microfluidic device with contactless liquid electrodes to isolate and enrich isolate and enrich a cell population (Fig. 5b).[56] They investigated the DEP response of live and dead THP-1 human leukemia monocytes under various electrical experimental conditions and further reported a 95% removal efficiency of viable THP-1 cells from dead ones.

The geometry of the insulating barrier between the sample and the electrodes can be customized to create a device that presents a high sensitivity towards specific cells. Salmanzadeh et al. developed and customized a contactless DEP device to separate prostate tumor-initiating cells (TICs) from regular tumor cells based on their dielectrophoretic properties (Fig. 5c).[57] Moreover, Zellner et al. reported another type of contactless DEP device, an off-chip passivated-electrode insulator-based DEP microchip (OπDEP, Fig. 5d), [143] capable of generating DEP forces which are larger by two orders of magnitude for the same applied voltage than the previous iDEP reported in the literature. Parallel metal electrodes were fabricated onto the device to produce a DEP force which allowed for high flow rates exceeding 1 ml/h. A100-μm-thick cover glass substrate acts as the insulating barrier between the metal electrodes and the main channel, which makes the metal electrodes reusable. With this device, Escherichia coli was isolated from polystyrene beads at 60% and 100% efficiency when the flow rate was 1.2 ml/h and 0.4 ml/h, respectively.

It is worth noting that both the geometry and materials used in contactless DEP devices have a significant impact on the frequency and the magnitude of the electric field gradient within the channel. Sano et al. studied the effects of geometry on the development of electric field gradients across a wide frequency spectrum and fabricated a low-frequency contactless DEP device to isolate human leukemia cells from dilute blood samples (Fig. 5e).[144] The electric field gradient was applied across a wide range of the frequency spectrum under 100 kHz, resulting in continuous isolation of cancer cells from a large number of red blood cells. Additionally, the DEP system can be manipulated by controlling the location of liquid metal electrodes and operating conditions can, hence, be determined by modifying the DEP force and the friction forces. Gwon et al. developed a movable liquid-drop DEP system for effective manipulation of yeast cells by actively controlling the location of an electrically conductive liquid metal that is used as the electrode instead of patterned surface electrodes. [145] With this system, they were able to demonstrate the active manipulation of yeast cells and measured both the collection efficiency and the dielectrophoretic velocity for different AC electric field strengths and applied frequencies. This DEP system is advantageous due to its ability to control the local position at which the particles can be collected by properly manipulating a liquid drop.

3.2. Patterned electrodes

In DEP devices, the electrodes through which an electric field is applied can be fabricated using either solid or liquid materials. Conventionally, electrodes were designed and manufactured using costly and sophisticated manufacturing methods that restrict their shape and area, limiting high throughput capabilities and device sensitivity. Additionally, numerous methods and techniques have been utilized to fabricate microelectrodes such as soft lithography, wet etching, traditional machining, hot embossing, laser ablation, plasma etching, and reactive ion etching.[146] However, photolithography is considered the foundation of all the processes. Metals such as gold, platinum, and copper are commonly utilized for solid electrodes. Kang et al. fabricated embedded-copper electrodes for a DEP device to generate a localized non-uniform AC electric field that is capable of separating yeast cells from polystyrene particles.[147] Other materials such as silver-polydimethylsiloxane (AgPDMS), ionic liquid, and oil emulsion are also used for fabricating electrodes.[53, 127, 148] Based on the structures of electrodes, DEP devices can be categorized into angled-electrode DEP devices and parallel/perpendicular-electrode DEP devices (Fig. 2).

3.2.1 Angled electrodes—In angled-electrode DEP devices, electrodes are parallel and angled on the top and bottom of a microfluidic channel. Angled electrodes generate an electric field gradient to change the direction of cell movement by a DEP force, and different cells may have different displacements due to their distinct DEP properties.[149] Typically, angled-electrode DEP devices have two pairs of electrodes on the bottom surface and the top surface of the main channel. If an electric field is applied at nDEP frequency in angled-electrode DEP devices, dielectric bioparticles that are in the vicinity of the electrode pair are repelled from the edges of electrodes. Therefore, the maximum F_{DEP} exerted by the nDEP barrier on a spherical bioparticle can be approximated by:[150–151]

$$F_{DEP} = \frac{27}{32}\pi^2\varepsilon_m Re\left(\frac{\varepsilon_p^* - \varepsilon_m^*}{\varepsilon_p^* + 2\varepsilon_m^*}\right)V^2\frac{r^3}{h^3} \tag{23}$$

where V is the applied electrical potential, and h is the height of the microchannel. Moreover, there is drag force on bioparticles in the medium, which is a viscous Stokes flow with a small Reynolds number can be calculated as follows:[152–153]

$$F_{Drag} = 6\pi\mu r(u_p - u_m) \tag{24}$$

where μ is the viscosity of the medium, and u_p and u_m are the speed of the bioparticle and the surrounding medium, respectively. In the main channel, the movement of bioparticles is driven by both the DEP and drag forces.

Hu et al. developed a DEP device with angled electrodes for marker-specific sorting of rare cells (Fig. 6a).[154] The electrodes were designed and fabricated on the device at an angle to the direction of the flow in order to reduce the nDEP force that is required to deflect the sample. With angled electrodes, rare cells with dielectrophoretic responsive labels are electrokinetically directed into the collection channel while rejecting unlabeled cells. It is worth noting that the performance of this device is governed by the balance between the F_{DEP} and the hydrodynamic forces (F_{HD}) on the labeled cells (Fig. 6a). In the same manner,

Pommer et al. conducted a size-dependent separation of platelets from diluted whole blood in an angled-electrode DEP device by tuning the device to deflect all larger cells such as red blood cells while keeping the smaller cells (i.e. platelets) in the collection channel (Fig. 6b).[155] Moreover, by implementing the architecture of the device with variable electrode angles and several outlets, it is possible to isolate a mixture of cells into multiple subpopulations within a particular cell division phase. Kim et al. reported the use of the dielectrophoresis phenomenon for a size-dependent selection of mammalian cancer cells based on their cell-cycle phase using an angled-electrode DEP device (Fig. 6c).[156] The device operates in the negative DEP regime by physically repelling cells away from higher electric field regions, based on their volume and their phase in the cell cycle, into weaker electric field regions. Angled electrodes have been used in both 3D and planar forms for cell trapping,[157–158] sorting,[159–160] and particle focusing.[161–162] However, the performance of angled electrodes-based microfluidic devices relies on several factors including the geometrical properties and the working conditions such as channel height, electrode angle, spacing between electrodes and their width, and the voltage applied.[163]

Dalili et al. further examined the effect of the width and length of the microchannel, the deflection angle of the electrodes, the sample volume, and the particle size on the performance of the angled-electrode-based system.[164] Using a linear model and statistical analysis to determine the significance of each factor on the particles, they concluded that except the channel width, all the factors they studied have a major effect on the DEP-induced displacement of particles. Kralj et al. developed an analytical model to predict the lateral displacement of the particles as a result of the hydrodynamic drag and DEP forces.[165] In agreement with their experimental data, they concluded that the length of the microchannel, voltage, particle size, and flow rate have a major effect on the particle displacement in the main channel. It is worth noting that this model did not consider the height and width of the microchannel or the deflection angle of the electrodes that are important factors in particle manipulation using an angled electrodes-based system. Importantly, angled electrodes in addition to their ability to attract/repel dielectric bioparticles by directing them to different outlets based on their distinct DEP properties,[166–167] can be used to generate a lateral force in a microfluidic channel.[168–169] This force is necessary for separating a mixture of bioparticles into distinct populations while achieving a high degree of spatial separation[149, 163] Hence they are very promising for non-invasive and label-free bioparticle manipulation.

3.2.2 Parallel/perpendicular electrodes—Parallel/perpendicular-electrode DEP devices, including changing-phase DEP devices and constant-phase DEP devices, typically have more than one pair of electrodes that are parallel to each other and perpendicular or parallel to the main channel. Changing-phase DEP is often called traveling-wave DEP (twDEP), where the phases of the voltage of different electrodes are different. This generates a continuous force acting on cells, and different cells will gain different acceleration and velocity due to their different DEP properties.

If the electric field phase gradient is not zero, cells will experience a DEP force even though there is no electric field intensity gradient in the main channel. Therefore, in the changing-phase DEP devices, the DEP force has two parts as shown in eq. (7). One part is due to the

electric field intensity gradient, which is given by the left part of the eq. (7) The other part is the traveling-wave DEP force due to the electric field phase gradient, which is proportional to the out-of-phase component of the induced dipole moment and the square of the field magnitude and can be calculated as follow:[83, 170]

$$F_{twDEP} = -\frac{4\pi^2 \varepsilon_m r^3}{\lambda} Im\left(\frac{\varepsilon_p^* - \varepsilon_m^*}{\varepsilon_p^* + 2\varepsilon_m^*}\right)|\boldsymbol{E}|^2 \quad (25)$$

where λ is the wavelength of the traveling electric field which is equal to the repetitive distance between the electrodes of the same phase.[103, 171] As shown in Fig. 7a, Cheng et al. fabricated a continuous 3D traveling-wave DEP device, which was used to separate red blood cells from debris-filled heterogeneous samples.[172] Constant-phase DEP devices can be divided into two types based on the separation mechanisms: one captures targeted cells and lets the remaining cells pass through the devices relying on different DEP responses of bioparticles or cells, while the other type actuates different cells into different layers in terms of height or streamlines due to different DEP responses of the bioparticles or cells.[78] Li et al. conducted a DEP separation of live and heat-treated Listeria innocua cells using interdigitated electrodes, achieving a separation efficiency of ~90% (Fig. 7b).[173] This device takes advantage of the difference in dielectric constant between dead and live cells. Therefore, as the frequency increases, the DEP for live cells changes to positive, and they are captured at the edges of electrodes while dead cells experience nDEP and are at the center of the electrodes. The pDEP can be used to attract cells toward the high electric field at the electrodes. Since the electric field intensity along with its non-uniformity decreases with increasing distance from the electrodes, the nDEP can then be used to trap cells in a stable position at a distance away from the electrodes. Rousselet et al. reported a DEP device to levitate and separate erythrocytes and latex beads using field-flow fractionation (Fig. 7c).[174] Parallel gold interdigitated microelectrodes were fabricated onto the device and by changing the frequency, the erythrocytes were attracted to the electrodes by pDEP while the latex beads were levitated above electrodes by nDEP.

Numerical studies have shown that differential sidewall electrodes not only prevent the need to apply high DC dielectrophoretic voltages but also decrease the Joule heating effect. Shirmohammadli et al. have manufactured differential sidewall gold electrodes into a microfluidic device channel and achieved 100% collection efficiency of cancer cells from blood cells.[175] By introducing sidewall electrodes, they were able to reduce the applied DC potential to 3 V and observed a significant decrease in Joule heating as a result of the reduced applied voltage. Nonspecific adherence of bioparticles on the electrodes is one of the limitations that complicate DEP-based microfluidic devices. To overcome this pitfall, Choi et al. reported the first microfluidic device for particle separation and analysis based on a trapezoidal electrodes array (TEA).[176–177] In this study, TEA is used as a source of negative DEP, which generates an electric field gradient along the perpendicular direction to fluid flow. This unique design allows for a continuous separation and analysis of different bioparticles based on their dielectric properties with improved recovery and selectivity while eliminating the nonspecific adherence of bioparticles onto the electrodes.

Other studies have used silver-based interdigitated electrodes due to their inhomogeneous two-layer structure, which creates a highly non-uniform electric field that can separate cells not only laterally but also vertically along the channel depth. Nie et al. demonstrated the use of AgPDMS to construct 3D microelectrodes for continuous-flow dielectrophoretic cell separation (Fig. 7d).[178] During the continuous separation, cells undergo an attraction by a pDEP force onto the gold electrode tips while those under nDEP force are repelled down to a lower position. Parallel/perpendicular-electrode DEP devices are very advantageous due to their simple structure and their straightforward microfabrication which facilitates efficient bioparticle manipulation.[179] Furthermore, with these types of electrodes, DEP force can be customized by modifying the electrode spacing or width.[148, 180–181] However, the large gap region between the electrodes can have some disadvantages such as a weak electric field in the regions that are further away from the electrodes, which leads to a relatively low DEP trapping efficiency.[182] Consequently, the low trapping forces in the main channel can limit the flow rate that can be used, therefore restricting the throughput of the device.[183] This limitation can be overcome by introducing a separate flow zone and capture zone in the main channel[71] which can minimize the impact of high flow speeds and the force in the flow zones on the capture efficiency.

3.3. Patterned media

Since the electric field distribution is dependent on the electric conductivity of the DEP media, DEP manipulation may be achieved by controlling the conductivity distribution of the DEP media to create an electric field gradient. For cell studies, the osmotic pressure of the DEP medium should be similar to that of the solution inside cells. Therefore, the concentration of electrolytes (which contribute to both the osmotic pressure and the conductivity) and/or sugars (which contribute to the osmotic pressure), may be varied to adjust both the osmotic pressure and the conductivity of the DEP medium (i.e., pattern the DEP medium).

Two different ways to pattern the DEP media have been explored (Fig. 2). Some studies used multiple types of DEP media of different electrical conductivities, such as multiple aqueous solutions with various concentrations of electrolytes flowing in different layers, in a device to control the electric field distribution. This takes advantage of the laminar nature of microfluidic flows with minimal mixing. Moreover, some materials (e.g., oil emulsion) with very different electric properties from water were used as DEP media for the manipulation of bioparticles.[53–54] Sun et al. developed an electric-conductivity gradient-induced DEP microfluidic device for continuous separation of different human cells.[127] In this study, two different types of DEP buffers (original versus modified) with different conductivities were used to generate a strong electric field gradient in the main channel (Fig. 8a). Vahey et al. developed an equilibrium method for continuous-flow cell sorting using multiple types of DEP media of various conductivities (Fig. 8b).[21] Angled metal electrodes were used to generate an electric field gradient and guide the cells in the direction of decreasing medium conductivity until the DEP force becomes sufficiently small that it is overwhelmed by hydrodynamic drag and the barrier is breached to allow cell collection. The conductivity gradient modulates DEP to achieve sorting of multiple particles in parallel. Huang et al. fabricated a DEP device to achieve extraction of cell-laden hydrogel microcapsules from an

oil phase into an aqueous solution (Fig. 8c),[53] where oil emulsion and aqueous solution were used as the two different DEP media of very different conductivities in the electrode region.

4. Outlook and Summary

The electric field (intensity or phase) gradient is a crucial factor for DEP manipulation of bioparticles, especially live cells, and can be generated by patterning the microchannels, electrodes, and media, individually or together in a DEP microfluidic device. This review categorizes current DEP devices based on the method of generating electric field gradients. In each category, various DEP devices have been developed for the manipulation of cells, depending on the requirements and conditions of specific applications. These devices present great potential for bioparticle manipulation although their throughput might be further improved. Additionally, new materials such as carbon electrodes,[184–187] liquid metal electrodes,[188] along with new manufacturing methods such as screen-printing,[189] and three dimensional (3D) printing,[190–192] may be developed to further improve the performance of DEP techniques; because the PDMS or glass used for making nearly all the devices reported so far can limit the integration of the electrodes.

More recently, optically induced DEP (oDEP) has emerged as a promising DEP technique for cell manipulation in microfluidic systems. With this technique, light is projected onto a photoconductive surface forming virtual electrodes, and they generate a local non-uniform electric field in the solution layer between the bottom and the top substrates.[193–194] This leads to the electric polarization of cells that are usually suspended in the solution layer. Unlike traditional DEP devices in which electrodes are fixed in one position, the oDEP possesses several advantages such as its non-contact cell manipulation and its simple manufacturing and operation. Furthermore, its electrode layout can be easily created or modified through the control of optical patterns, therefore acting as virtual electrodes.[195] The oDEP technique also allows for a quick modification of the electrode set up through the control of optical images which contributes to a more flexible manipulation of the cells.[196–197]

This method has been successfully applied to different cells and applications such as circulating tumor cells purification[198] and isolation[199] with higher performance than the conventional counterparts. Furthermore, this technique has the potential to be integrated with other microfluidic separation methods to further enhance the purification processes.[200] For instance, it has been integrated with fluorescence technique in which the fluorescence dye was used to differentiate the targeted cell from surrounding cells followed by implementation of oDEP to isolate live CTCs from the blood with 100% purity which is higher than conventional techniques.[200] Its integration with other methods would help to improve the cell isolating/sorting purity of each method alone, especially for those that are based on negative selection to isolate cancer cells from blood.[162, 201] For the negative selection methods, blood cells are targeted for removal, leaving behind cancer cells in the sample. For example, Chiu et al. integrated the oDEP with a laminar flow in a microfluidic system to achieve almost 100% CTC purity from blood.[202] The group designed a microfluidic system with a T-shaped channel in which a moving light bar was utilized to selectively transport leucocytes to the side of the microchannel for collection without

deflecting cancer cells. Under an oDEP field, a smaller light image was used to generate a more focused electric field which contributed to the higher oDEP manipulation force. This force was subsequently used for highly efficient CTC isolation from patient blood with purity as high as 100%.

Another important advantage of oDEP is the capability of achieving high resolution with low optical intensity.[203] Moreover, the oDEP can be driven by different conditions such as the magnitude and frequency of the applied AC voltage.[193, 204–205] However, the biological cells being separated are prone to random aggregation due to the electric fields in the main channel, which could hinder the use of oDEP force to effectively separate the two cell species. To overcome this hurdle, Huang et al. designed an aggregation-free oDEP system to separate cancer cells from leucocytes based on their differences in size and electric properties.[203] In addition to varying the AC voltages with different magnitudes (2–7 V) and frequencies (50–1500 kHz), the group used a charge-coupled device (CCD) camera-equipped microscope to track and record the dynamic movement of cell aggregation in the main channel. They then used the voltage that generated the least aggregation to isolate viable cancer cells that were spiked in a leukocyte suspension with a recovery rate and purity of more than 76% and 74%, respectively. The recovery rate is the percentage of the isolated cancer cell number over the spiked cancer cell number while the purity (%) is defined as the percentage of the isolated cancer cell number over the total collected cell number.

Compared to the conventional biochemical methods with antibodies, the specificity of DEP-based manipulation of bioparticles may not be as high. Therefore, the combination of DEP with biochemical methods may facilitate the widespread application of the DEP-based microfluidic manipulation of bioparticles, including living cells, in the fields of stem cell technology, cancer detection and therapy, drug delivery, and environmental safety. It is worth noting that a combination of both passive and active methods may overcome their individual weaknesses and maximize the benefits of both methods.[206] Passive methods like the biochemical methods take advantage of the channel geometry or other intrinsic hydrodynamic phenomena and do not require an external field whereas active methods involve the utilization of external fields.[207] Therefore, DEP integration with other manipulation methods can enable more powerful functionality to achieve both higher purity and capturing/sorting/separating efficiency.

Lately, several studies have reported the integration of DEP with other passive methods such as hydrophoresis, a newly emerging hydrodynamic particle focusing method that takes advantage of the steric effects between particles and grooves, to improve separation efficiency.[208–212] DEP has also been integrated with inertial microfluidics, a method that uses inertial force to separate cells in a laminar flow,[42–46, 213–214] to improve throughput and separation efficiency and purity.[215–217] Other studies have also combined DEP with viscoelastic focusing,[218–219] flow fractionation,[162, 220–222], deterministic lateral displacement,[223–226] and machine learning[227], to achieve improved separation efficiency and purity. As an active method, DEP has also been used in tandem with other active cell manipulation methods including magnetophoresis,[228–230] optical tweezers,[231–233] and acoustofluidics[234–239] to improve the versatility and performance of the device.

Furthermore, this integration is important to achieve both augmented throughput and sensitivity that are crucial for point-of-care applications.

DEP-based microfluidic devices have consistently been shown to be promising for label-free separation, characterization, and manipulation of bioparticles including living cells. However, there remains issue stemming from insufficient capability of cell isolation/characterization with high throughput. For DEP-based microfluidic devices to be applicable in a commercial setting, this pitfall needs to be overcome. Integrating DEP with other methods as aforementioned may be a promising strategy to address this pitfall. Furthermore, the majority of DEP-based microfluidic devices are made of PDMS which is a relatively high-cost material in comparison to the widely used and more accessible industry-standard materials such as cyclic olefin copolymer (COC), polymethyl methacrylate (PMMA), polystyrene (PA), and polycarbonate.[240] Furthermore, PDMS presents more disadvantages due to its hydrophobic surface and tendency to swell in organic solvents.[241] Therefore, more studies are needed for improving the throughput and achieving low-cost fabrication of DEP devices to facilitate their commercial uses.

It is worth noting that despite these challenges, DEP-based microfluidic devices continue to evolve in numerous fields. A number of DEP-based microfluidic devices have been successfully incorporated into the commercial settings. For example, the Panasonic bacteria counter which uses the changes in impedance between electrodes to measure bacterial concentration.[242] The Silicon Biosystems DEPArray uses electrodes to generate an electric field around cells, which enables image-based isolation of single cells.[243] Additional DEP-based microfluidic devices that are integrated with different techniques including the Shimadzu IG-1000 nanoparticle analyzer, DEPtech,[244–245] and ApoStream system,[222, 246] have successfully attained commercial labels.

In summary, DEP force may be generated for bioparticle manipulation based on the patterns of microchannels, electrodes, and media. DEP-based microfluidic devices are promising tools for bioparticle manipulation such as sorting, focusing, trapping, and cell isolation/capture with applications in medicine, pharmaceutics, biology, and chemistry. Their attractiveness continues to rise due to their ability to manipulate bioparticles including various biological cells based on their geometric parameters and physicochemical properties. DEP-based microfluidic systems have been widely studied, particularly in academic research settings, and they may be further improved in terms of throughput, specificity, complexity, and cost. This may be done by combining DEP with other approaches and making DEP devices with new materials, to facilitate their wide applications in both academic and industrial settings

Acknowledgments

This work was partially supported by grants from the American Cancer Society (ACS #120936-RSG-11-109-01-CDD) and NIH (R01EB023632, R01CA206366, R01CA243023, and R01AI123661).

References

(1). Lagus TP; Edd JF, A Review of the Theory, Methods and Recent Applications of High-Throughput Single-Cell Droplet Microfluidics. J. of Phys. D: Appl. Phys 2013, 46 (11), 114005. 10.1088/0022-3727/46/11/114005.

(2). Zhang Q; Austin RH, Applications of Microfluidics in Stem Cell Biology. J. Bionanosci 2012, 2 (4), 277–286. 10.1007/s12668-012-0051-8.

(3). Park D; Lim J; Park JY; Lee S-H, Concise Review: Stem Cell Microenvironment on a Chip: Current Technologies for Tissue Engineering and Stem Cell Biology. Stem. Cells Transl. Med 2015, 4 (11), 1352–1368. 10.5966/sctm.2015-0095. [PubMed: 26450425]

(4). Ertl P; Sticker D; Charwat V; Kasper C; Lepperdinger G, Lab-on-a-Chip Technologies for Stem Cell Analysis. Trends Biotechnol 2014, 32 (5), 245–253. 10.1016/j.tibtech.2014.03.004. [PubMed: 24726257]

(5). Wang G; McCain ML; Yang L; He A; Pasqualini FS; Agarwal A; Yuan H; Jiang D; Zhang D; Zangi L; Geva J; Roberts AE; Ma Q; Ding J; Chen J; Wang D-Z; Li K; Wang J; Wanders RJA; Kulik W; Vaz FM; Laflamme MA; Murry CE; Chien KR; Kelley RI; Church GM; Parker KK; Pu WT, Modeling the Mitochondrial Cardiomyopathy of Barth Syndrome with Induced Pluripotent Stem Cell and Heart-on-Chip Technologies. Nat. Med 2014, 20 (6), 616–623. 10.1038/nm.3545. [PubMed: 24813252]

(6). Warren L; Ni Y; Wang J; Guo X, Feeder-Free Derivation of Human Induced Pluripotent Stem Cells with Messenger RNA. Sci. Rep 2012, 2, 657–657. 10.1038/srep00657. [PubMed: 22984641]

(7). Kulik W; van Lenthe H; Stet FS; Houtkooper RH; Kemp H; Stone JE; Steward CG; Wanders RJ; Vaz FM, Bloodspot Assay Using HPLC-Tandem Mass Spectrometry for Detection of Barth Syndrome. Clin. Chem 2008, 54 (2), 371. 10.1373/clinchem.2007.095711. [PubMed: 18070816]

(8). Bhatia SN; Ingber DE, Microfluidic Organs-on-Chips. Nat. Biotechnol 2014, 32, 760. 10.1038/nbt.2989. [PubMed: 25093883]

(9). He M; Zeng Y, Microfluidic Exosome Analysis toward Liquid Biopsy for Cancer. J. Lab. Autom 2016, 21 (4), 599–608. 10.1177/2211068216651035. [PubMed: 27215792]

(10). Chen J; Li J; Sun Y, Microfluidic Approaches for Cancer Cell Detection, Characterization, and Separation. Lab Chip 2012, 12 (10), 1753–1767. 10.1039/C2LC21273K. [PubMed: 22437479]

(11). Murlidhar V; Rivera-Báez L; Nagrath S, Affinity Versus Label-Free Isolation of Circulating Tumor Cells: Who Wins? Small 2016, 12 (33), 4450–4463. 10.1002/smll.201601394. [PubMed: 27436104]

(12). Damiati S; Kompella UB; Damiati SA; Kodzius R, Microfluidic Devices for Drug Delivery Systems and Drug Screening. Genes 2018, 9 (2), 103. 10.3390/genes9020103.

(13). Tran TH; Nguyen CT; Kim D-P; Lee Y.-k.; Huh KM, Microfluidic Approach for Highly Efficient Synthesis of Heparin-Based Bioconjugates for Drug Delivery. Lab Chip 2012, 12 (3), 589–594. 10.1039/C1LC20769E. [PubMed: 22134726]

(14). Hassan S; Zhang YS, Chapter 10 - Microfluidic Technologies for Local Drug Delivery. In Microfluid. Pharm. Appl, Santos HA; Liu D; Zhang H, Eds. William Andrew Publishing: 2019; pp 281–305. 10.1016/B978-0-12-812659-2.00010-7.

(15). Almeida MIGS; Jayawardane BM; Kolev SD; McKelvie ID, Developments of Microfluidic Paper-Based Analytical Devices (μPADs) for Water Analysis: A Review. Talanta 2018, 177, 176–190. 10.1016/j.talanta.2017.08.072. [PubMed: 29108573]

(16). Luque de Castro MD, Chapter 8 - Membrane-Based Separation Techniques: Dialysis, Gas Diffusion and Pervaporation. In Compr. Anal. Chem, Kolev SD; McKelvie ID, Eds. Elsevier: 2008; Vol. 54, pp 203–234. 10.1016/S0166-526X(08)00608-9.

(17). Cardoso TMG; Garcia PT; Coltro WKT, Colorimetric Determination of Nitrite in Clinical, Food and Environmental Samples Using Microfluidic Devices Stamped in Paper Platforms. Anal. Methods 2015, 7 (17), 7311–7317. 10.1039/C5AY00466G.

(18). Carrell C; Kava A; Nguyen M; Menger R; Munshi Z; Call Z; Nussbaum M; Henry C, Beyond the Lateral Fow Asay: A Review of Paper-Based Microfluidics. Microelectron. Eng 2019, 206, 45–54. 10.1016/j.mee.2018.12.002.

(19). Busa LSA; Mohammadi S; Maeki M; Ishida A; Tani H; Tokeshi M, Advances in Microfluidic Paper-Based Analytical Devices for Food and Water Analysis. Micromachines 2016, 7 (5), 86. 10.3390/mi7050086.

(20). Jokerst JC; Emory JM; Henry CS, Advances in Microfluidics for Environmental Analysis. Analyst 2012, 137 (1), 24–34. 10.1039/C1AN15368D. [PubMed: 22005445]

(21). Vahey MD; Voldman J, An Equilibrium Method for Continuous-Flow Cell Sorting Using Dielectrophoresis. Anal. Chem 2008, 80 (9), 3135–3143. 10.1021/ac7020568. [PubMed: 18363383]

(22). Baret JC; Miller OJ; Taly V; Ryckelynck M; El-Harrak A; Frenz L; Rick C; Samuels ML; Hutchison JB; Agresti JJ; Link DR; Weitz DA; Griffiths AD, Fluorescence-Activated Droplet Sorting (FADS): Eificient Microfluidic Cell Sorting Based on Enzymatic Activity. Lab Chip 2009, 9 (13), 1850–1858. 10.1039/B902504a. [PubMed: 19532959]

(23). Wang MM; Tu E; Raymond DE; Yang JM; Zhang HC; Hagen N; Dees B; Mercer EM; Forster AH; Kariv I; Marchand PJ; Butler WF, Microfluidic Sorting of Mammalian Cells by Optical Force Switching. Nat. Biotechnol 2005, 23 (1), 83–87. 10.1038/Nbt1050. [PubMed: 15608628]

(24). Pamme N; Wilhelm C, Continuous Sorting of Magnetic Cells Via On-Chip Free-Flow Magnetophoresis. Lab Chip 2006, 6 (8), 974–980. 10.1039/B604542a. [PubMed: 16874365]

(25). Han KH; Frazier AB, Paramagnetic Capture Mode Magnetophoretic Microseparator for High Efficiency Blood Cell Separations. Lab Chip 2006, 6 (2), 265–273. 10.1039/B514539b. [PubMed: 16450037]

(26). Murthy SK; Sin A; Tompkins RG; Toner M, Effect of Flow and Surface Conditions on Human Lymphocyte Isolation Using Microfluidic Chambers. Langmuir 2004, 20 (26), 11649–11655. 10.1021/La048047b. [PubMed: 15595794]

(27). Nagrath S; Sequist LV; Maheswaran S; Bell DW; Irimia D; Ulkus L; Smith MR; Kwak EL; Digumarthy S; Muzikansky A; Ryan P; Balis UJ; Tompkins RG; Haber DA; Toner M, Isolation of Rare Circulating Tumour Cells in Cancer Patients by Microchip Technology. Nature 2007, 450 (7173), 1235–U10. 10.1038/Nature06385. [PubMed: 18097410]

(28). Hymer WC; Barlow GH; Blaisdell SJ; Cleveland C; Farrington MA; Feldmeier M; Grindeland R; Hatfield JM; Lanham JW; Lewis ML; Morrison DR; Olack BJ; Richman DW; Rose J; Scharp DW; Snyder RS; Swanson CA; Todd P; Wilfinger W, Continuous-Flow Electrophoretic Separation of Proteins and Cells from Mammalian-Tissues. Cell Biophys 1987, 10 (1), 61–85. 10.1007/BF02797074 [PubMed: 2440579]

(29). Todd P; Plank LD; Kunze ME; Lewis ML; Morrison DR; Barlow GH; Lanham JW; Cleveland C, Electrophoretic Separation and Analysis of Living Cells from Solid Tissues by Several Methods - Human-Embryonic Kidney-Cell-Cultures as a Model. J. Chromatogr 1986, 364, 11–24. 10.1016/S0021-9673(00)96191-0. [PubMed: 3771695]

(30). Hansen E; Hannig K, Electrophoretic Separation of Lymphoid-Cells. Method. Enzymol 1984, 108, 180–197. 10.1016/s0076-6879(84)08085-x

(31). MacDonald MP; Spalding GC; Dholakia K, Microfluidic Sorting in an Optical Lattice. Nature 2003, 426 (6965), 421–424. 10.1038/Nature02144. [PubMed: 14647376]

(32). Shi JJ; Huang H; Stratton Z; Huang YP; Huang TJ, Continuous Particle Separation in a Microfluidic Channel via Standing Surface Acoustic Waves (SSAW). Lab Chip 2009, 9 (23), 3354–3359. 10.1039/B915113c. [PubMed: 19904400]

(33). Petersson F; Aberg L; Sward-Nilsson AM; Laurell T, Free Flow Acoustophoresis: Microfluidic-Based Mode of Particle and Cell Separation. Anal. Chem 2007, 79 (14), 5117–5123. 10.1021/Ac070444e. [PubMed: 17569501]

(34). Ozcelik A; Rufo J; Guo F; Gu Y; Li P; Lata J; Huang TJ, Acoustic Tweezers for the Life Sciences. Nat. Methods 2018, 15 (12), 1021–1028. 10.1038/s41592-018-0222-9. [PubMed: 30478321]

(35). Davis JA; Inglis DW; Morton KJ; Lawrence DA; Huang LR; Chou SY; Sturm JC; Austin RH, Deterministic Hydrodynamics: Taking Blood Apart. Proc. Natl. Acad. Sci. U.S.A 2006, 103 (40), 14779–14784. 10.1073/Pnas.0605967103. [PubMed: 17001005]

(36). Wilding P; Kricka LJ; Cheng J; Hvichia G; Shoffner MA; Fortina P, Integrated Cell Isolation and Polymerase Chain Reaction Analysis Using Silicon Microfilter Chambers. Anal. Biochem 1998, 257 (2), 95–100. 10.1006/Abio.1997.2530. [PubMed: 9514776]

(37). Tan SJ; Yobas L; Lee GYH; Ong CN; Lim CT, Microdevice for the Isolation and Enumeration of Cancer Cells from Blood. Biomed. Microdevices 2009, 11 (4), 883–892. 10.1007/S10544-009-9305-9. [PubMed: 19387837]

(38). Chen X; Cui DF; Liu CC; Li H, Microfluidic Chip for Blood Cell Separation and Collection Based on Crossflow Filtration. Sens. Actuators, B 2008, 130 (1), 216–221. 10.1016/J.Snb.2007.07.126.

(39). Yamada M; Nakashima M; Seki M, Pinched Flow Fractionation: Continuous Size Separation of Particles Utilizing a Laminar Flow Profile in a Pinched Microchannel. Anal. Chem 2004, 76 (18), 5465–71. 10.1021/ac049863r. [PubMed: 15362908]

(40). Takagi J; Yamada M; Yasuda M; Seki M, Continuous Particle Separation in a Microchannel Having Asymmetrically Arranged Multiple Branches. Lab Chip 2005, 5 (7), 778–784. 10.1039/B501885d. [PubMed: 15970972]

(41). Yamada M; Seki M, Hydrodynamic Filtration for On-Chip Particle Concentration and Classification Utilizing Microfluidics. Lab Chip 2005, 5 (11), 1233–1239. 10.1039/B509386d. [PubMed: 16234946]

(42). Park JS; Song SH; Jung HI, Continuous Focusing of Microparticles Using Inertial Lift Force and Vorticity via Multi-Orifice Microfluidic Channels. Lab Chip 2009, 9 (7), 939–948. 10.1039/B813952k. [PubMed: 19294305]

(43). Di Carlo D; Irimia D; Tompkins RG; Toner M, Continuous Inertial Focusing, Ordering, and Separation of Particles in Microchannels. Proc. Natl. Acad. Sci. U.S.A 2007, 104 (48), 18892–18897. 10.1073/Pnas.0704958104. [PubMed: 18025477]

(44). Di Carlo D; Edd JF; Irimia D; Tompkins RG; Toner M, Equilibrium Separation and Filtration of Particles Using Differential Inertial Focusing. Anal. Chem 2008, 80 (6), 2204–2211. 10.1021/Ac702283m. [PubMed: 18275222]

(45). Kuntaegowdanahalli SS; Bhagat AAS; Kumar G; Papautsky I, Inertial Microfluidics for Continuous Particle Separation in Spiral Microchannels. Lab Chip 2009, 9 (20), 2973–2980. 10.1039/B908271a. [PubMed: 19789752]

(46). Wu ZG; Willing B; Bjerketorp J; Jansson JK; Hjort K, Soft Inertial Microfluidics for High Throughput Separation of Bacteria from Human Blood Cells. Lab Chip 2009, 9 (9), 1193–1199. 10.1039/B817611f. [PubMed: 19370236]

(47). Agarwal P; Zhao S; Bielecki P; Rao W; Choi JK; Zhao Y; Yu J; Zhang W; He X, One-Step Microfluidic Generation of Pre-Hatching Embryo-Like Core-Shell Microcapsules for Miniaturized 3D Culture of Pluripotent Stem Cells. Lab Chip 2013, 13 (23), 4525–33. 10.1039/c3lc50678a. [PubMed: 24113543]

(48). Choi JK; Agarwal P; Huang H; Zhao S; He X, The Crucial Role of Mechanical Heterogeneity in Regulating Follicle Development and Ovulation with Engineered Ovarian Microtissue. Biomaterials 2014, 35 (19), 5122–8. 10.1016/j.biomaterials.2014.03.028. [PubMed: 24702961]

(49). Zhang W; Yang G; Zhang A; Xu LX; He X, Preferential Vitrification of Water in Small Alginate Microcapsules Significantly Augments Cell Cryopreservation by Vitrification. Biomed. Microdevices 2010, 12 (1), 89–96. 10.1007/s10544-009-9363-z. [PubMed: 19787454]

(50). Lee KY; Mooney DJ, Hydrogels for Tissue Engineering. Chem. Rev. (Washington, DC, U. S.) 2001, 101 (7), 1869–79. 10.1021/cr000108x.

(51). Kim C; Chung S; Kim YE; Lee KS; Lee SH; Oh KW; Kang JY, Generation of Core-Shell Microcapsules with Three-Dimensional Focusing Device for Efficient Formation of Cell Spheroid. Lab Chip 2011, 11 (2), 246–52. 10.1039/c0lc00036a. [PubMed: 20967338]

(52). Zhang W; He X, Microencapsulating and Banking Living Cells for Cell-Based Medicine. J. Healthc. Eng 2011, 2 (4), 427–446. 10.1260/2040-2295.2.4.427. [PubMed: 22180835]

(53). Huang H; Sun M; Heisler-Taylor T; Kiourti A; Volakis J; Lafyatis G; He X, Stiffness-Independent Highly Efficient On-Chip Extraction of Cell-Laden Hydrogel Microcapsules from Oil Emulsion into Aqueous Solution by Dielectrophoresis. Small 2015, 11 (40), 5369–5374. 10.1002/smll.201501388. [PubMed: 26297051]

(54). Sun M; Durkin P; Li J; Toth TL; He X, Label-Free On-Chip Selective Extraction of Cell-Aggregate-Laden Microcapsules from Oil into Aqueous Solution with Optical Sensor and Dielectrophoresis. ACS Sens 2018, 3 (2), 410–417. 10.1021/acssensors.7b00834. [PubMed: 29299919]

(55). Huang H; He X, Interfacial Tension Based On-Chip Extraction of Microparticles Confined in Microfluidic Stokes Flows. Appl. Phys. Lett 2014, 105, 143704. 10.1063/1.4898040. [PubMed: 25378709]

(56). Shafiee H; Sano MB; Henslee EA; Caldwell JL; Davalos RV, Selective Isolation of Live/Dead Cells Using Contactless Dielectrophoresis (cDEP). Lab Chip 2010, 10 (4), 438–445. 10.1039/B920590j. [PubMed: 20126683]

(57). Salmanzadeh A; Romero L; Shafiee H; Gallo-Villanueva RC; Stremler MA; Cramer SD; Davalos RV, Isolation of Prostate Tumor Initiating Cells (TICS) Through Their Dielectrophoretic Signature. Lab Chip 2012, 12 (1), 182–189. 10.1039/C1lc20701f. [PubMed: 22068834]

(58). Alinezhadbalalami N; Douglas TA; Balani N; Verbridge SS; Davalos RV, The Feasibility of Using Dielectrophoresis for Isolation of Glioblastoma Subpopulations with Increased Stemness. Electrophoresis 2019, 40 (18–19), 2592–2600. 10.1002/elps.201900026. [PubMed: 31127957]

(59). Alshareef M; Metrakos N; Juarez Perez E; Azer F; Yang F; Yang X; Wang G, Separation of Tumor Cells with Dielectrophoresis-Based Microfluidic Chip. Biomicrofluidics 2013, 7 (1), 11803. 10.1063/1.4774312. [PubMed: 24403985]

(60). Natu R; Islam M; Martinez-Duarte R, Nondimensional Streaming Dielectrophoresis Number for a System of Continuous Particle Separation. Anal. Chem 2019, 91 (7), 4357–4367. 10.1021/acs.analchem.8b04599. [PubMed: 30827100]

(61). Yang F; Yang X; Jiang H; Wang G, Cascade and Staggered Dielectrophoretic Cell Sorters. Electrophoresis 2011, 32 (17), 2377–84. 10.1002/elps.201100039. [PubMed: 21823131]

(62). Natu R; Islam M; Keck D; Martinez-Duarte R, Automated “Pick and Transfer” of Targeted Cells Using Dielectrophoresis. Lab Chip 2019, 19 (15), 2512–2525. 10.1039/c9lc00409b. [PubMed: 31259984]

(63). Bhagat AA; Bow H; Hou HW; Tan SJ; Han J; Lim CT, Microfluidics for Cell Separation. Med. Biol. Eng. Comput 2010, 48 (10), 999–1014. 10.1007/s11517-010-0611-4. [PubMed: 20414811]

(64). Li M; Li WH; Zhang J; Alici G; Wen W, A Review of Microfabrication Techniques and Dielectrophoretic Microdevices for Particle Manipulation and Separation. J. Phys. D: Appl. Phys 2014, 47 (6), 063001. 10.1088/0022-3727/47/6/063001.

(65). Pethig R, Review Article-Dielectrophoresis: Status of the Theory, Technology, and Applications. Biomicrofluidics 2010, 4 (2), 022811. 10.1063/1.3456626. [PubMed: 20697589]

(66). Kim D; Sonker M; Ros A, Dielectrophoresis: From Molecular to Micrometer-Scale Analytes. Anal. Chem 2019, 91 (1), 277–295. 10.1021/acs.analchem.8b05454. [PubMed: 30482013]

(67). Demircan Y; Özgür E; Külah H, Dielectrophoresis: Applications and Future Outlook in Point of Care. Electrophoresis 2013, 34 (7), 1008–1027. 10.1002/elps.201200446. [PubMed: 23348714]

(68). Yang J; Huang Y; Wang X-B; Becker FF; Gascoyne PRC, Differential Analysis of Human Leukocytes by Dielectrophoretic Field-Flow-Fractionation. Biophys. J 2000, 78 (5), 2680–2689. 10.1016/S0006-3495(00)76812-3. [PubMed: 10777764]

(69). Yildizhan Y; Erdem N; Islam M; Martinez-Duarte R; Elitas M, Dielectrophoretic Separation of Live and Dead Monocytes Using 3D Carbon-Electrodes. Sensors) 2017, 17 (11). 10.3390/s17112691.

(70). Srivastava SK; Daggolu PR; Burgess SC; Minerick AR, Dielectrophoretic Characterization of Erythrocytes: Positive ABO Blood Types. Electrophoresis 2008, 29 (24), 5033–5046. 10.1002/elps.200800166. [PubMed: 19130588]

(71). Sun M; Xu J; Shamul JG; Lu X; Husain S; He X, Creating a Capture Zone in Microfluidic Flow Greatly Enhances the Throughput and Efficiency of Cancer Detection. Biomaterials 2019, 197, 161–170. 10.1016/j.biomaterials.2019.01.014. [PubMed: 30660052]

(72). Adams TNG; Jiang AYL; Vyas PD; Flanagan LA, Separation of Neural Stem Cells by Whole Cell Membrane Capacitance Using Dielectrophoresis. Methods 2018, 133, 91–103. 10.1016/j.ymeth.2017.08.016. [PubMed: 28864355]

(73). Cummings EB; Singh AK, Dielectrophoresis on Microchips Containing Arrays of Insulating Posts: Theoretical and Experimental Results. Anal. Chem 2003, 75 (18), 4724–4731. 10.1021/ac0340612. [PubMed: 14674447]

(74). Hawkins BG; Smith AE; Syed YA; Kirby BJ, Continuous-Flow Particle Separation by 3D Insulative Dielectrophoresis Using Coherently Shaped, DC-Biased, AC Electric Fields. Anal. Chem 2007, 79 (19), 7291–7300. 10.1021/ac0707277. [PubMed: 17764153]

(75). Velev OD; Bhatt KH, On-Chip Micromanipulation and Assembly of Colloidal Particles by Electric Fields. Soft Matter 2006, 2 (9), 738–750. 10.1039/B605052B. [PubMed: 32680214]

(76). Nili H; Green NG, AC Electrokinetics of Nanoparticles. In Encycl. Nanotechnol, Bhushan B, Ed. Springer Netherlands: Dordrecht, 2016; pp 1–10. 10.1007/978-94-007-6178-0_130-2.

(77). Gangwal S; Cayre OJ; Velev OD, Dielectrophoretic Assembly of Metallodielectric Janus Particles in AC Electric Fields. Langmuir 2008, 24 (23), 13312–13320. 10.1021/la8015222. [PubMed: 18973307]

(78). Gascoyne PRC; Vykoukal J, Particle Separation by Dielectrophoresis. Electrophoresis 2002, 23 (13), 1973–1983. 10.1002/1522-2683(200207)23:13<1973::AID-ELPS1973>3.0.CO;2-1. [PubMed: 12210248]

(79). Amah E; Janjua M; Singh P, Direct Numerical Simulation of Particles in Spatially Varying Electric Fields. Fluids 2018, 3 (3). 10.3390/fluids3030052.

(80). Hill N; Lapizco-Encinas BH, Continuous Flow Separation of Particles with Insulator-Based Dielectrophoresis Chromatography. Anal. Bioanal. Chem 2020. 10.1007/s00216-019-02308-w.

(81). Zhao K; Larasati; Duncker BP; Li D, Continuous Cell Characterization and Separation by Microfluidic Alternating Current Dielectrophoresis. Anal. Chem 2019, 91 (9), 6304–6314. 10.1021/acs.analchem.9b01104. [PubMed: 30977369]

(82). D'Amico L; Ajami NJ; Adachi JA; Gascoyne PRC; Petrosino JF, Isolation and Concentration of Bacteria from Blood Using Microfluidic Membraneless Dialysis and Dielectrophoresis. Lab Chip 2017, 17 (7), 1340–1348. 10.1039/C6LC01277A. [PubMed: 28276545]

(83). Wang XB; Huang Y; Becker FF; Gascoyne PRC, A Unified Theory of Dielectrophoresis and Traveling-Wave Dielectrophoresis. J. Phys. D: Appl. Phys 1994, 27 (7), 1571–1574. DOI:10.1088/0022-3727/27/7/036.

(84). Pesch GR; Du F, A Review of Dielectrophoretic Separation and Classification of Non-Biological Particles. Electrophoresis 2020, 42, 134–152. 10.1002/elps.202000137. [PubMed: 32667696]

(85). Pohl HA; Pollock K; Crane JS, Dielectrophoretic Force: A Comparison of Theory and Experiment. J. Biol. Phys 1978, 6 (3), 133–160. 10.1007/BF02328936.

(86). Pysher MD; Hayes MA, Electrophoretic and Dielectrophoretic Field Gradient Technique for Separating Bioparticles. Anal. Chem 2007, 79 (12), 4552–4557. 10.1021/Ac070534j. [PubMed: 17487977]

(87). Lapizco-Encinas BH; Simmons BA; Cummings EB; Fintschenko Y, Dielectrophoretic Concentration and Separation of Live and Dead Bacteria in an Array of Insulators. Anal. Chem 2004, 76 (6), 1571–1579. 10.1021/ac034804j [PubMed: 15018553]

(88). Weiss NG; Jones PV; Mahanti P; Chen KP; Taylor TJ; Hayes MA, Dielectrophoretic Mobility Determination in DC Insulator-Based Dielectrophoresis. Electrophoresis 2011, 32 (17), 2292–2297. 10.1002/elps.201100034. [PubMed: 21823129]

(89). King MR; Lomakin OA; Ahmed R; Jones TB, Size-Selective Deposition of Particles Combining Liquid and Particulate Dielectrophoresis. J. Appl. Phys 2005, 97 (5). 10.1063/1.1852694.

(90). Wang XB; Yang J; Huang Y; Vykoukal J; Becker FF; Gascoyne PR, Cell Separation by Dielectrophoretic Field-Flow-Fractionation. Anal. Chem 2000, 72 (4), 832–839. 10.1021/ac990922o. [PubMed: 10701270]

(91). Bazant MZ; Ben Y, Theoretical Prediction of Fast 3D AC Electro-Osmotic Pumps. Lab Chip 2006, 6 (11), 1455–1461. 10.1039/B608092H. [PubMed: 17066170]

(92). Shin JH; Kim K; Woo H; Kang IS; Kang H-W; Choi W; Lim G, One-Directional Flow of Ionic Solutions Along Fine Electrodes Under an Alternating Current Electric Field. R. Soc. Open Sci 2019, 6 (2), 180657. 10.1098/rsos.180657. [PubMed: 30891253]

(93). Modarres P; Tabrizian M, Alternating Current Dielectrophoresis of Biomacromolecules: The Interplay of Electrokinetic Effects. Sens. Actuators B 2017, 252, 391–408. 10.1016/j.snb.2017.05.144.

(94). Gagnon ZR, Cellular Dielectrophoresis: Applications to the Characterization, Manipulation, Separation and Patterning of Cells. Electrophoresis 2011, 32 (18), 2466–2487. 10.1002/elps.201100060. [PubMed: 21922493]

(95). Ji-Ping H; Kin-Wah Y; Jun L; Hong S, Spectral Representation Theory for Dielectric Behavior of Nonspherical Cell Suspensions. Commun. Theor. Phys 2002, 38 (1), 113–120. 10.1088/0253-6102/38/1/113.

(96). Yang CY; Lei U, Quasistatic Force and Torque on Ellipsoidal Particles Under Generalized Dielectrophoresis. J. Appl. Phys 2007, 102 (9), 094702. 10.1063/1.2802185.

(97). Huang Y; Holzel R; Pethig R; Wang X-B, Differences in the AC Electrodynamics of Viable and Non-Viable Yeast Cells Determined Through Combined Dielectrophoresis and Electrorotation Studies. Phys. Med. Biol 1992, 37 (7), 1499–1517. 10.1088/0031-9155/37/7/003. [PubMed: 1631195]

(98). LaLonde A; Romero-Creel MF; Saucedo-Espinosa MA; Lapizco-Encinas BH, Isolation and Enrichment of Low Abundant Particles with Insulator-Based Dielectrophoresis. Biomicrofluidics 2015, 9 (6), 064113. 10.1063/1.4936371. [PubMed: 26674134]

(99). Madiyar FR; Haller SL; Farooq O; Rothenburg S; Culbertson C; Li J, AC Dielectrophoretic Manipulation and Electroporation of Vaccinia Virus Using Carbon Nanoelectrode Arrays. Electrophoresis 2017, 38 (11), 1515–1525. 10.1002/elps.201600436. [PubMed: 28211116]

(100). Han S-I; Lee S-M; Joo Y-D; Han K-H, Lateral Dielectrophoretic Microseparators to Measure the Size Distribution of Blood Cells. Lab Chip 2011, 11 (22), 3864–3872. 10.1039/C1LC20413K. [PubMed: 21964758]

(101). Siebman C; Velev OD; Slaveykova VI, Two-Dimensional Algal Collection and Assembly by Combining AC-Dielectrophoresis with Fluorescence Detection for Contaminant-Induced Oxidative Stress Sensing. Biosensors 2015, 5 (2). 10.3390/bios5020319.

(102). Gallo-Villanueva RC; Jesús-Pérez NM; Martínez-López JI; Pacheco A; Lapizco-Encinas BH, Assessment of Microalgae Viability Employing Insulator-Based Dielectrophoresis. Microfluid. Nanofluid 2011, 10 (6), 1305–1315. 10.1007/s10404-010-0764-3.

(103). Qian C; Huang H; Chen L; Li X; Ge Z; Chen T; Yang Z; Sun L, Dielectrophoresis for Bioparticle Manipulation. Int. J. Mol. Sci 2014, 15 (10). 10.3390/ijms151018281.

(104). Jaffe A; Voldman J, Multi-Frequency Dielectrophoretic Characterization of Single Cells. Microsyst. Nanoeng 2018, 4 (1), 23. 10.1038/s41378-018-0023-4. [PubMed: 31057911]

(105). P. R. C, G.; J. V, V., Dielectrophoresis-Based Sample Handling in General-Purpose Programmable Diagnostic Instruments. Proc. IEEE 2004, 92 (1), 22–42. 10.1109/JPROC.2003.820535.

(106). Chan KL; Gascoyne PRC; Becker FF; Pethig R, Electrorotation of Liposomes: Verification of Dielectric Multi-Shell Model for Cells. Biochim. Biophys. Acta, Lipids Lipid Metab 1997, 1349 (2), 182–196. 10.1016/S0005-2760(97)00092-1.

(107). Su H-W; Prieto JL; Voldman J, Rapid Dielectrophoretic Characterization of Single Cells Using the Dielectrophoretic Spring. Lab Chip 2013, 13 (20), 4109–4117. 10.1039/C3LC50392E. [PubMed: 23970334]

(108). Ibsen SD; Wright J; Lewis JM; Kim S; Ko S-Y; Ong J; Manouchehri S; Vyas A; Akers J; Chen CC; Carter BS; Esener SC; Heller MJ, Rapid Isolation and Detection of Exosomes and Associated Biomarkers from Plasma. ACS Nano 2017, 11 (7), 6641–6651. 10.1021/acsnano.7b00549. [PubMed: 28671449]

(109). Frusawa H, Frequency-Modulated Wave Dielectrophoresis of Vesicles and Cells: Periodic U-Turns at the Crossover Frequency. Nanoscale Res. Lett 2018, 13 (1), 169. 10.1186/s11671-018-2583-5. [PubMed: 29881976]

(110). Irimajiri A; Hanai T; Inouye A, A Dielectric Theory of “Multi-Stratified Shell” Model with Its Application to a Lymphoma Cell. J. Theor. Biol 1979, 78 (2), 251–269. 10.1016/0022-5193(79)90268-6. [PubMed: 573830]

(111). Rohani A; Moore JH; Kashatus JA; Sesaki H; Kashatus DF; Swami NS, Label-Free Quantification of Intracellular Mitochondrial Dynamics Using Dielectrophoresis. Anal. Chem 2017, 89 (11), 5757–5764. 10.1021/acs.analchem.6b04666. [PubMed: 28475301]

(112). Becker FF; Wang XB; Huang Y; Pethig R; Vykoukal J; Gascoyne PRC, The Removal of Human Leukaemia Cells from Blood Using Interdigitated Microelectrodes. J. Phys. D: Appl. Phys 1994, 27 (12), 2659–2662. 10.1088/0022-3727/27/12/030.

(113). Mahaworasilpa TL; Coster HGL; George EP, Forces on Biological Cells Due to Applied Alternating (AC) Electric-Fields .1. Dielectrophoresis. Biochim. Biophys. Acta, Biomembr 1994, 1193 (1), 118–126. 10.1016/0005-2736(94)90340-9

(114). Nguyen N-V; Le Manh T; Nguyen TS; Le VT; Van Hieu N, Applied Electric Field Analysis and Numerical Investigations of the Continuous Cell Separation in a Dielectrophoresis-Based Microfluidic Channel. J. Sci: Adv. Mater. Devices 2021, 6 (1), 11–18. 10.1016/j.jsamd.2020.11.002.

(115). Zhelev DV; Needham D, 4 - The Influence of Electric Fields on Biological and Model Membranes. Biol. Eff. Electr. Magn. Fields Carpenter DO; Ayrapetyan S, Eds. Academic Press: San Diego, 1994; pp 105–142. 10.1016/B978-0-12-160261-1.50009-2.

(116). Aldaeus F; Lin Y; Roeraade J; Amberg G, Superpositioned Dielectrophoresis for Enhanced Trapping Efficiency. Electrophoresis 2005, 26 (22), 4252–4259. 10.1002/elps.200500068. [PubMed: 16240293]

(117). Srivastava SK; Gencoglu A; Minerick AR, DC Insulator Dielectrophoretic Applications in Microdevice Technology: A Review. Anal. Bioanal. Chem 2011, 399 (1), 301–321. 10.1007/S00216-010-4222-6. [PubMed: 20967429]

(118). Lapizco-Encinas BH; Simmons BA; Cummings EB; Fintschenko Y, Insulator-Based Dielectrophoresis for the Selective Concentration and Separation of Live Bacteria in Water. Electrophoresis 2004, 25 (10–11), 1695–1704. 10.1002/elps.200405899 [PubMed: 15188259]

(119). Lapizco-Encinas BH; Davalos RV; Simmons BA; Cummings EB; Fintschenko Y, An Insulator-Based (Electrodeless) Dielectrophoretic Concentrator for Microbes in Water. J. Microbiol. Meth 2005, 62 (3), 317–326. 10.1016/j.mimet.2005.04.027

(120). Kang YJ; Li DQ; Kalams SA; Eid JE, DC-Dielectrophoretic Separation of Biological Cells by Size. Biomed. Microdevices 2008, 10 (2), 243–249. 10.1007/s10544-007-9130-y [PubMed: 17899384]

(121). Jones PV; Staton SJR; Hayes MA, Blood Cell Capture in a Sawtooth Dielectrophoretic Microchannel. Anal. Bioanal. Chem 2011, 401 (7), 2103. 10.1007/s00216-011-5284-9. [PubMed: 21830138]

(122). Jones PV; DeMichele AF; Kemp L; Hayes MA, Differentiation of Escherichia Coli Serotypes Using DC Gradient Insulator Dielectrophoresis. Anal. Bioanal. Chem 2014, 406 (1), 183–192. 10.1007/s00216-013-7437-5. [PubMed: 24202194]

(123). Barbulovic-Nad I; Xuan XC; Lee JSH; Li DQ, DC-Dielectrophoretic Separation of Microparticles Using an Oil Droplet Obstacle. Lab Chip 2006, 6 (2), 274–279. 10.1039/B513183A [PubMed: 16450038]

(124). Srivastava SK; Artemiou A; Minerick AR, Direct Current Insulator-Based Dielectrophoretic Characterization of Erythrocytes: ABO-Rh Human Blood Typing. Electrophoresis 2011, 32 (18), 2530–2540. 10.1002/elps.201100089 [PubMed: 21922495]

(125). Tang S-Y; Zhu J; Sivan V; Gol B; Soffe R; Zhang W; Mitchell A; Khoshmanesh K, Creation of Liquid Metal 3D Microstructures Using Dielectrophoresis. Adv. Funct. Mater 2015, 25 (28), 4445–4452. 10.1002/adfm.201501296.

(126). So J-H; Dickey MD, Inherently Aligned Microfluidic Electrodes Composed of Liquid Metal. Lab Chip 2011, 11 (5), 905–911. 10.1039/C0LC00501K. [PubMed: 21264405]

(127). Sun MR; Agarwal P; Zhao ST; Zhao Y; Lu XB; He XM, Continuous On-Chip Cell Separation Based on Conductivity-Induced Dielectrophoresis with 3D Self-Assembled Ionic Liquid Electrodes. Anal. Chem 2016, 88 (16), 8264–8271. 10.1021/acs.analchem.6b02104. [PubMed: 27409352]

(128). Kikkeri K; Kerr BA; Bertke AS; Strobl JS; Agah M, Passivated-Electrode Insulator-Based Dielectrophoretic Separation of Heterogeneous Cell Mixtures. J. Sep. Sci 2020, 43 (8), 1576–1585. 10.1002/jssc.201900553. [PubMed: 31991043]

(129). Mohammadi M; Madadi H; Casals-Terré J; Sellarès J, Hydrodynamic and Direct-Current Insulator-Based Dielectrophoresis (H-DC-IDEP) Microfluidic Blood Plasma Separation. Anal. Bioanal. Chem 2015, 407 (16), 4733–4744. 10.1007/s00216-015-8678-2. [PubMed: 25925854]

(130). Zhou T; Ge J; Shi L; Fan J; Liu Z; Woo Joo S, Dielectrophoretic Choking Phenomenon of a Deformable Particle in a Converging-Diverging Microchannel. Electrophoresis 2018, 39 (4), 590–596. 10.1002/elps.201700250. [PubMed: 29193170]

(131). Ai Y; Joo SW; Jiang Y; Xuan X; Qian S, Transient Electrophoretic Motion of a Charged Particle Through a Converging-Diverging Microchannel: Effect of Direct Current-Dielectrophoretic Force. Electrophoresis 2009, 30 (14), 2499–2506. 10.1002/elps.200800792. [PubMed: 19639572]

(132). Ai Y; Qian S; Liu S; Joo SW, Dielectrophoretic Choking Phenomenon in a Converging-Diverging Microchannel. Biomicrofluidics 2010, 4 (1), 013201. 10.1063/1.3279787.

(133). Chen KP; Pacheco JR; Hayes MA; Staton SJR, Insulator-Based Dielectrophoretic Separation of Small Particles in a Sawtooth Channel. Electrophoresis 2009, 30 (9), 1441–1448. 10.1002/elps.200800833. [PubMed: 19425000]

(134). Zhou T; Ji X; Shi L; Zhang X; Deng Y; Joo SW, Dielectrophoretic Choking Phenomenon in a Converging-Diverging Microchannel for Janus Particles. Electrophoresis 2019, 40 (6), 993–999. 10.1002/elps.201800368. [PubMed: 30371959]

(135). Zhu J; Xuan X, Dielectrophoretic Focusing of Particles in a Microchannel Constriction Using DC-Biased AC Flectric Fields. Electrophoresis 2009, 30 (15), 2668–2675. 10.1002/elps.200900017. [PubMed: 19621378]

(136). Hyoung Kang K; Xuan X; Kang Y; Li D, Effects of DC-Dielectrophoretic Force on Particle Trajectories in Microchannels. J. Appl. Phys 2006, 99 (6), 064702. 10.1063/1.2180430.

(137). Kang Y; Cetin B; Wu Z; Li D, Continuous Particle Separation with Localized AC-Dielectrophoresis Using Embedded Electrodes and an Insulating Hurdle. Electrochim. Acta 2009, 54 (6), 1715–1720. 10.1016/j.electacta.2008.09.062.

(138). Park S; Koklu M; Beskok A, Particle Trapping in High-Conductivity Media with Electrothermally Enhanced Negative Dielectrophoresis. Anal. Chem 2009, 81 (6), 2303–2310. 10.1021/ac802471g. [PubMed: 19215119]

(139). Du J-R; Juang Y-J; Wu J-T; Wei H-H, Long-Range and Superfast Trapping of DNA Molecules in an AC Electrokinetic Funnel. Biomicrofluidics 2008, 2 (4), 044103. 10.1063/1.3037326.

(140). Cheng IF; Chang H-C; Hou D; Chang H-C, An Integrated Dielectrophoretic Chip for Continuous Bioparticle Filtering, Focusing, Sorting, Trapping, and Detecting. Biomicrofluidics 2007, 1 (2), 021503. 10.1063/1.2723669.

(141). Alshareef M; Metrakos N; Juarez Perez E; Azer F; Yang F; Yang X; Wang G, Separation of Tumor Cells with Dielectrophoresis-Based Microfluidic Chip. Biomicrofluidics 2013, 7 (1), 011803. 10.1063/1.4774312.

(142). Shafiee H; Caldwell JL; Sano MB; Davalos RV, Contactless Dielectrophoresis: A New Technique for Cell Manipulation. Biomed. Microdevices 2009, 11 (5), 997–1006. 10.1007/s10544-009-9317-5 [PubMed: 19415498]

(143). Zellner P; Shake T; Sahari A; Behkam B; Agah M, Off-Chip Passivated-Electrode, Insulator-Based Dielectrophoresis (OPIDEP). Anal. Bioanal. Chem 2013, 405 (21), 6657–66. 10.1007/s00216-013-7123-7. [PubMed: 23812879]

(144). Sano MB; Caldwell JL; Davalos RV, Modeling and Development of a Low Frequency Contactless Dielectrophoresis (CDEP) Platform to Sort Cancer Cells from Dilute Whole Blood Samples. Biosens. Bioelectron 2011, 30 (1), 13–20. 10.1016/j.bios.2011.07.048 [PubMed: 21944186]

(145). Gwon HR; Chang ST; Choi CK; Jung J-Y; Kim J-M; Lee SH, Development of a New Contactless Dielectrophoresis System for Active Particle Manipulation Using Movable Liquid Electrodes. Electrophoresis 2014, 35 (14), 2014–2021. 10.1002/elps.201300566. [PubMed: 24737601]

(146). Fiorini GS; Chiu DT, Disposable Microfluidic Devices: Fabrication, Function, and Application. BioTechniques 2005, 38 (3), 429–446. 10.2144/05383RV02. [PubMed: 15786809]

(147). Kang YJ; Cetin B; Wu ZM; Li DQ, Continuous Particle Separation with Localized AC-Dielectrophoresis Using Embedded Electrodes and an Insulating Hurdle. Electrochim. Acta 2009, 54 (6), 1715–1720. 10.1016/j.electacta.2008.09.062

(148). Lewpiriyawong N; Kandaswamy K; Yang C; Ivanov V; Stocker R, Microfluidic Characterization and Continuous Separation of Cells and Particles Using Conducting Poly(Dimethyl Siloxane) Electrode Induced Alternating Current-Dielectrophoresis. Anal. Chem 2011, 83 (24), 9579–9585. 10.1021/ac202137y. [PubMed: 22035423]

(149). Yunus NAM; Green NG, Continuous Separation of Submicron Particles Using Angled Electrodes. J. Phys. Conf. Ser 2008, 142, 012068. 10.1088/1742-6596/142/1/012068.

(150). Durr M; Kentsch J; Muller T; Schnelle T; Stelzle M, Microdevices for Manipulation and Accumulation of Micro and Nanoparticles by Dielectrophoresis. Electrophoresis 2003, 24 (4), 722–731. 10.1002/elps.200390087 [PubMed: 12601744]

(151). Schnelle T; Müller T; Fiedler S; Fuhr G, The Influence of Higher Moments on Particle Behaviour in Dielectrophoretic Field Cages. J. Electrost 1999, 46 (1), 13–28. 10.1016/S0304-3886(98)00055-2.

(152). Voldman J, Dielectrophoretic Traps for Cell Manipulation. BioMEMS Biomed. Nanotechnol: Vol. IV: Biomolecular Sensing, Processing and Analysis, Ferrari M; Bashir R; Wereley S, Eds. Springer US: Boston, MA, 2007; pp 159–186. 10.1007/978-0-387-25845-4_8.

(153). Salmanzadeh A; Kittur H; Sano MB; Roberts C, P.; Schmelz EM; Davalos RV, Dielectrophoretic Differentiation of Mouse Ovarian Surface Epithelial Cells, Macrophages, and Fibroblasts Using Contactless Dielectrophoresis. Biomicrofluidics 2012, 6 (2), 024104. 10.1063/1.3699973.

(154). Hu XY; Bessette PH; Qian JR; Meinhart CD; Daugherty PS; Soh HT, Marker-Specific Sorting of Rare Cells Using Dielectrophoresis. Proc. Natl. Acad. Sci. U.S.A 2005, 102 (44), 15757–15761. 10.1073/Pnas.0507719102. [PubMed: 16236724]

(155). Pommer MS; Zhang YT; Keerthi N; Chen D; Thomson JA; Meinhart CD; Soh HT, Dielectrophoretic Separation of Platelets from Diluted Whole Blood in Microfluidic Channels. Electrophoresis 2008, 29 (6), 1213–1218. 10.1002/Elps.200700607. [PubMed: 18288670]

(156). Kim U; Shu CW; Dane KY; Daugherty PS; Wang JYJ; Soh HT, Selection of Mammalian Cells Based on Their Cell-Cycle Phase Using Dielectrophoresis. Proc. Natl. Acad. Sci. U.S.A 2007, 104 (52), 20708–20712. 10.1073/Pnas.0708760104. [PubMed: 18093921]

(157). Wu Y; Ren Y; Tao Y; Hou L; Jiang H, High-Throughput Separation, Trapping, and Manipulation of Single Cells and Particles by Combined Dielectrophoresis at a Bipolar Electrode Array. Anal. Chem 2018, 90 (19), 11461–11469. 10.1021/acs.analchem.8b02628. [PubMed: 30192521]

(158). Das D; Biswas K; Das S, A Microfluidic Device for Continuous Manipulation of Biological Cells Using Dielectrophoresis. Med. Eng. Phys 2014, 36 (6), 726–731. 10.1016/j.medengphy.2013.12.010. [PubMed: 24388100]

(159). Han S-I; Huang C; Han A, In-Droplet Cell Separation Based on Bipolar Dielectrophoretic Response to Facilitate Cellular Droplet Assays. Lab Chip 2020, 20 (20), 3832–3841. 10.1039/D0LC00710B. [PubMed: 32926042]

(160). Han K-H; Han S-I; Frazier AB, Lateral Displacement as a Function of Particle Size Using a Piecewise Curved Planar Interdigitated Electrode Array. Lab Chip 2009, 9 (20), 2958–2964. 10.1039/B909753H. [PubMed: 19789750]

(161). Song H; Rosano JM; Wang Y; Garson CJ; Prabhakarpandian B; Pant K; Klarmann GJ; Perantoni A; Alvarez LM; Lai E, Continuous-Flow Sorting of Stem Cells and Differentiation Products Based on Dielectrophoresis. Lab Chip 2015, 15 (5), 1320–1328. 10.1039/C4LC01253D. [PubMed: 25589423]

(162). Moon H-S; Kwon K; Kim S-I; Han H; Sohn J; Lee S; Jung H-I, Continuous Separation of Breast Cancer Cells from Blood Samples Using Multi-Orifice Flow Fractionation (MOFF) and Dielectrophoresis (DEP). Lab Chip 2011, 11 (6), 1118–1125. 10.1039/C0LC00345J. [PubMed: 21298159]

(163). Dalili A; Taatizadeh E; Tahmooressi H; Tasnim N; Rellstab-Sánchez PI; Shaunessy M; Najjaran H; Hoorfar M, Parametric Study on the Geometrical Parameters of a Lab-on-a-chip Platform with Tilted Planar Electrodes for Continuous Dielectrophoretic Manipulation of Microparticles. Sci. Rep 2020, 10 (1), 11718. 10.1038/s41598-020-68699-4. [PubMed: 32678180]

(164). Dalili A; Montazerian H; Sakthivel K; Tasnim N; Hoorfar M, Dielectrophoretic Manipulation of Particles on a Microfluidics Platform with Planar Tilted Electrodes. Sens. Actuators, B 2021, 329, 129204. 10.1016/j.snb.2020.129204.

(165). Kralj JG; Lis MTW; Schmidt MA; Jensen KF, Continuous Dielectrophoretic Size-Based Particle Sorting. Anal. Chem 2006, 78 (14), 5019–5025. 10.1021/ac0601314. [PubMed: 16841925]

(166). Kazemi B; Darabi J, Numerical Simulation of Dielectrophoretic Particle Separation Using Slanted Electrodes. Phys. Fluids 2018, 30 (10), 102003. 10.1063/1.5047153.

(167). Tajik P; Saidi MS; Kashaninejad N; Nguyen N-T, Simple, Cost-Effective, and Continuous 3D Dielectrophoretic Microchip for Concentration and Separation of Bioparticles. Ind. Eng. Chem. Res 2020, 59 (9), 3772–3783. 10.1021/acs.iecr.9b00771.

(168). Hadady H; Redelman D; Hiibel R, S.; Geiger J, E., Continuous-Flow Sorting of Microalgae Cells Based on Lipid Content by High Frequency Dielectrophoresis. AIMS Biophys 2016, 3 (3), 398–414. 10.3934/biophy.2016.3.398.

(169). Md Yunus NA; Abidin ZZ, Characterization of Microelectrode Array of Dielectrophoretic Microfluidic Device. J. Bioeng. Biomed. Sci 2016, 6 (3). 10.4172/2155-9538.1000190.

(170). Morgan H; Izquierdo AG; Bakewell D; Green NG; Ramos A, The Dielectrophoretic and Travelling Wave Forces Generated by Interdigitated Electrode Arrays: Analytical Solution Using Fourier Series. J. Phys. D: Appl. Phys 2001, 34 (17), 2708–2708. 10.1088/0022-3727/34/10/316.

(171). Huang Y; Wang XB; Tame JA; Pethig R, Electrokinetic Behavior of Colloidal Particles in Traveling Electric Fields: Studies Using Yeast-Cells. J. Phys. D: Appl. Phys 1993, 26 (9), 1528–1535. 10.1088/0022-3727/26/9/030.

(172). Cheng IF; Froude VE; Zhu YX; Chang HC; Chang HC, A Continuous High-Throughput Bioparticle Sorter Based on 3D Traveling-Wave Dielectrophoresis. Lab Chip 2009, 9 (22), 3193–3201. 10.1039/B910587e. [PubMed: 19865725]

(173). Li HB; Bashir R, Dielectrophoretic Separation and Manipulation of Live and Heat-Treated Cells of Listeria on Microfabricated Devices with Interdigitated Electrodes. Sens. Actuators, B 2002, 86 (2–3), 215–221. 10.1016/S0925-4005(02)00172-7.

(174). Rousselet J; MArkx GH; Pethig R, Separation of Erythrocytes and Latex Beads by Dielectrophoretic Levitation and Hyperlayer Field-Flow Fractionation. Colloids Surf. A 1998, 140 (1–3), 209–216. 10.1016/S0927-7757(97)00279-3.

(175). Shirmohammadli V; Manavizadeh N, Application of Differential Electrodes in a Dielectrophoresis-Based Device for Cell Separation. IEEE Trans. Electron Devices 2019, 66 (9), 4075–4080. 10.1109/TED.2019.2926427.

(176). Choi S; Park J-K, Microfluidic System for Dielectrophoretic Separation Based on a Trapezoidal Electrode Array. Lab Chip 2005, 5 (10), 1161–1167. 10.1039/B505088J. [PubMed: 16175274]

(177). Sungyoung C; Park J Fabrication and Characterization of Trapezoidal Electrode Array for Dielectrophoretic Separation, Transducers ‘05, Int. Conf. Solid-State Sens., Actuators Microsyst., Dig. Tech. Pap., 13th, 2005; pp 1616–1619 Vol. 2. DOI: 10.1109/SENSOR.2005.1497397.

(178). Nie X; Zhang Z; Han C; Yu D; Xing X Dielectrophoretic Cell Separation Using Conducting Silver PDMS Microelectrodes Featuring Non-Uniform Sidewall Profile, IEEE Int. Conf. Micro Electro Mech. Syst., 32nd, 2019; pp 39–42. DOI: 10.1109/MEMSYS.2019.8870644.

(179). Lin JTY; Yeow JTW, Enhancing Dielectrophoresis Effect Through Novel Electrode Geometry. Biomed. Microdevices 2007, 9 (6), 823–831. 10.1007/s10544-007-9095-x. [PubMed: 17574532]

(180). Albrecht DR; Sah RL; Bhatia SN, Geometric and Material Determinants of Patterning Efficiency by Dielectrophoresis. Biophys. J 2004, 87 (4), 2131–2147. 10.1529/biophysj.104.039511. [PubMed: 15454417]

(181). Lewpiriyawong N; Yang C; Lam YC, Continuous Sorting and Separation of Microparticles by Size Using AC Dielectrophoresis in a PDMS Microfluidic Device with 3-D Conducting PDMS Composite Electrodes. Electrophoresis 2010, 31 (15), 2622–2631. 10.1002/elps.201000087. [PubMed: 20665920]

(182). Li M; Li S; Cao W; Li W; Wen W; Alici G, Improved Concentration and Separation of Particles in a 3D Dielectrophoretic Chip Integrating Focusing, Aligning and Trapping. Microfluid. Nanofluid 2013, 14 (3), 527–539. 10.1007/s10404-012-1071-y.

(183). Abt V; Gringel F; Han A; Neubauer P; Birkholz M, Separation, Characterization, and Handling of Microalgae by Dielectrophoresis. Microorganisms 2020, 8 (4), 540. 10.3390/microorganisms8040540.

(184). Yildizhan Y; Erdem N; Islam M; Martinez-Duarte R; Elitas M, Dielectrophoretic Separation of Live and Dead Monocytes Using 3D Carbon-Electrodes. Sensors 2017, 17 (11), 2691. 10.3390/s17112691.

(185). Elitas M; Martinez-Duarte R; Dhar N; McKinney JD; Renaud P, Dielectrophoresis-Based Purification of Antibiotic-Treated Bacterial Subpopulations. Lab Chip 2014, 14 (11), 1850–1857. 10.1039/C4LC00109E. [PubMed: 24756475]

(186). Martinez-Duarte R; Camacho-Alanis F; Renaud P; Ros A, Dielectrophoresis of Lambda-DNA Using 3D Carbon Electrodes. Electrophoresis 2013, 34 (7), 1113–1122. 10.1002/elps.201200447. [PubMed: 23348619]

(187). Jaramillo M. d. C.; Torrents E; Martínez-Duarte R; Madou MJ; Juárez A, On-Line Separation of Bacterial Cells by Carbon-Electrode Dielectrophoresis. Electrophoresis 2010, 31 (17), 2921–2928. 10.1002/elps.201000082. [PubMed: 20690146]

(188). Zhu B; Cai Y; Wu Z; Niu F; Yang H, Dielectrophoretic Microfluidic Chip Integrated with Liquid Metal Electrode for Red Blood Cell Stretching Manipulation. IEEE Access 2019, 7, 152224–152232. 10.1109/ACCESS.2019.2948191.

(189). Wee WH; Li Z; Hu J; Kadri NA; Xu F; Li F; Pingguan-Murphy B, Fabrication of Dielectrophoretic Microfluidic Chips Using a Facile Screen-Printing Technique for Microparticle Trapping. J.Micromech. Microeng 2015, 25 (10), 105015. 10.1088/0960-1317/25/10/105015.

(190). Teoh BY; Lee PF; Thong YL; Lim YM In Design of DC-Dielectrophoresis Microfluidic Channel for Particle and Biological Cell Separation Using 3D Printed PVA Material, 2018 IEEE-EMBS Conference on Biomedical Engineering and Sciences (IECBES), 3–6 Dec. 2018; 2018; pp 566–570. DOI: 10.1109/IECBES.2018.8626636.

(191). Au AK; Huynh W; Horowitz LF; Folch A, 3D-Printed Microfluidics. Angew. Chem. Int. Ed 2016, 55 (12), 3862–3881. 10.1002/anie.201504382.

(192). Philippin N; Frey A; Michatz M; Kuehne I, 3D-Printed Microfluidic Chip System for Dielectrophoretic Manipulation of Colloids. Proceed. 2018 COMSOL Confer., Lausanne, 2018.

(193). Chiu T-K; Chao AC; Chou W-P; Liao C-J; Wang H-M; Chang J-H; Chen P-H; Wu M-H, Optically-Induced-Dielectrophoresis (ODEP)-Based Cell Manipulation in a Microfluidic System for High-Purity Isolation of Integral Circulating Tumor Cell (CTC) Clusters Based on Their Size Characteristics. Sens. Actuators, B 2018, 258, 1161–1173. 10.1016/j.snb.2017.12.003.

(194). Hwang H; Park J-K, Optoelectrofluidic Platforms for Chemistry and Biology. Lab Chip 2011, 11 (1), 33–47. 10.1039/C0LC00117A. [PubMed: 20944856]

(195). Chiou PY; Ohta AT; Wu MC, Massively Parallel Manipulation of Single Cells and Microparticles Using Optical Images. Nature 2005, 436 (7049), 370–372. 10.1038/nature03831. [PubMed: 16034413]

(196). Lin Y-H; Yang Y-W; Chen Y-D; Wang S-S; Chang Y-H; Wu M-H, The Application of an Optically Switched Dielectrophoretic (ODEP) Force for the Manipulation and Assembly of Cell-Encapsulating Alginate Microbeads in a Microfluidic Perfusion Cell Culture System for Bottom-Up Tissue Engineering. Lab Chip 2012, 12 (6), 1164–1173. 10.1039/C2LC21097E. [PubMed: 22322420]

(197). Ohta AT; Garcia M; Valley JK; Banie L; Hsu H-Y; Jamshidi A; Neale SL; Lue T; Wu MC, Motile and Non-Motile Sperm Diagnostic Manipulation Using Optoelectronic Tweezers. Lab Chip 2010, 10 (23), 3213–3217. 10.1039/C0LC00072H. [PubMed: 20835428]

(198). Chiu T-K; Chou W-P; Huang S-B; Wang H-M; Lin Y-C; Hsieh C-H; Wu M-H, Application of Optically-Induced-Dielectrophoresis in Microfluidic System for Purification of Circulating Tumour Cells for Gene Expression Analysis-Cancer Cell Line Model. Sci. Rep 2016, 6, 32851–32851. 10.1038/srep32851. [PubMed: 27609546]

(199). Chou W-P; Wang H-M; Chang J-H; Chiu T-K; Hsieh C-H; Liao C-J; Wu M-H, The Utilization of Optically-Induced-Dielectrophoresis (ODEP)-Based Virtual Cell Filters in a Microfluidic System for Continuous Isolation and Purification of Circulating Tumour Cells (CTCS) Based on Their Size Characteristics. Sens. Actuators, B: 2017, 241, 245–254. 10.1016/j.snb.2016.10.075.

(200). Liao C-J; Hsieh C-H; Chiu T-K; Zhu Y-X; Wang H-M; Hung F-C; Chou W-P; Wu M-H, An Optically Induced Dielectrophoresis (ODEP)-Based Microfluidic System for the Isolation of High-Purity CD45(Neg)/EpCAM(Neg) Cells from the Blood Samples of Cancer Patients: Demonstration and Initial Exploration of the Clinical Significance of These Cells. Micromachines 2018, 9 (11), 563. 10.3390/mi9110563.

(201). Hou HW; Warkiani ME; Khoo BL; Li ZR; Soo RA; Tan DS-W; Lim W-T; Han J; Bhagat AAS; Lim CT, Isolation and Retrieval of Circulating Tumor Cells Using Centrifugal Forces. Sci. Rep 2013, 3, 1259–1259. 10.1038/srep01259. [PubMed: 23405273]

(202). Chiu T-K; Chou W-P; Huang S-B; Wang H-M; Lin Y-C; Hsieh C-H; Wu M-H, Application of Optically-Induced-Dielectrophoresis in Microfluidic System for Purification of Circulating Tumour Cells for Gene Expression Analysis: Cancer Cell Line Model. Sci. Rep 2016, 6 (1), 32851. 10.1038/srep32851. [PubMed: 27609546]

(203). Huang S-B; Wu M-H; Lin Y-H; Hsieh C-H; Yang C-L; Lin H-C; Tseng C-P; Lee G-B, High-Purity and Label-Free Isolation of Circulating Tumor Cells (CTCS) in a Microfluidic Platform by Using Optically-Induced-Dielectrophoretic (ODEP) Force. Lab Chip 2013, 13 (7), 1371–1383. 10.1039/C3LC41256C. [PubMed: 23389102]

(204). Chu P-Y; Hsieh C-H; Lin C-R; Wu M-H, The Effect of Optically Induced Dielectrophoresis (ODEP)-Based Cell Manipulation in a Microfluidic System on the Properties of Biological Cells. Biosensors 2020, 10 (6), 65. 10.3390/bios10060065.

(205). Liu N; Lin Y; Peng Y; Xin L; Yue T; Liu Y; Ru C; Xie S; Dong L; Pu H; Chen H; Li WJ; Sun Y, Automated Parallel Electrical Characterization of Cells Using Optically-Induced Dielectrophoresis. IEEE Trans. Autom. Sci. Eng 2020, 17 (2), 1084–1092. 10.1109/TASE.2019.2963044.

(206). Yan S; Zhang J; Yuan D; Li W, Hybrid Microfluidics Combined with Active and Passive Approaches for Continuous Cell Separation. Electrophoresis 2017, 38 (2), 238–249. 10.1002/elps.201600386. [PubMed: 27718260]

(207). Sajeesh P; Sen AK, Particle Separation and Sorting in Microfluidic Devices: A Review. Microfluid. Nanofluid 2014, 17 (1), 1–52. 10.1007/s10404-013-1291-9.

(208). Choi S; Park J-K, Continuous Hydrophoretic Separation and Sizing of Microparticles Using Slanted Obstacles in a Microchannel. Lab Chip 2007, 7 (7), 890–897. 10.1039/B701227F. [PubMed: 17594009]

(209). Yan S; Zhang J; Yuan Y; Lovrecz G; Alici G; Du H; Zhu Y; Li W, A Hybrid Dielectrophoretic and Hydrophoretic Microchip for Particle Sorting Using Integrated Prefocusing and Sorting Steps. Electrophoresis 2015, 36 (2), 284–291. 10.1002/elps.201400397. [PubMed: 25363719]

(210). Yan S; Zhang J; Pan C; Yuan D; Alici G; Du H; Zhu Y; Li W, An Integrated Dielectrophoresis-active Hydrophoretic Microchip for Continuous Particle Filtration and Separation. J.Micromech. Microeng 2015, 25 (8), 084010. 10.1088/0960-1317/25/8/084010.

(211). Yan S; Zhang J; Alici G; Du H; Zhu Y; Li W, Isolating Plasma from Blood Using a Dielectrophoresis-Active Hydrophoretic Device. Lab Chip 2014, 14 (16), 2993–3003. 10.1039/C4LC00343H. [PubMed: 24939716]

(212). Jiang AYL; Yale AR; Aghaamoo M; Lee D-H; Lee AP; Adams TNG; Flanagan LA, High-Throughput Continuous Dielectrophoretic Separation of Neural Stem Cells. Biomicrofluidics 2019, 13 (6), 064111. 10.1063/1.5128797. [PubMed: 31737160]

(213). Kim G-Y; Han J-I; Park J-K, Inertial Microfluidics-Based Cell Sorting. BioChip J.l 2018, 12 (4), 257–267. 10.1007/s13206-018-2401-2.

(214). Zhou Y; Ma Z; Ai Y, Sheathless Inertial Cell Focusing and Sorting with Serial Reverse Wavy Channel Structures. Microsyst. Nanoeng 2018, 4 (1), 5. 10.1038/s41378-018-0005-6. [PubMed: 31057895]

(215). Zhang J; Yuan D; Zhao Q; Yan S; Tang S-Y; Tan SH; Guo J; Xia H; Nguyen N-T; Li W, Tunable Particle Separation in a Hybrid Dielectrophoresis (DEP)-Inertial Microfluidic Device. Sens. Actuators, B 2018, 267, 14–25. 10.1016/j.snb.2018.04.020.

(216). Zhang J; Yan S; Alici G; Nguyen N-T; Di Carlo D; Li W, Real-Time Control of Inertial Focusing in Microfluidics Using Dielectrophoresis (DEP). RSC Adv 2014, 4 (107), 62076–62085. 10.1039/C4RA13075H.

(217). Wang Y; Wang J; Cheng J; Zhang Y; Ding G; Wang X; Chen M; Kang Y; Pan X, Serial Separation of Microalgae in a Microfluidic Chip Under Inertial and Dielectrophoretic Forces. IEEE Sens. J 2020, 20 (24), 14607–14616. 10.1109/JSEN.2020.3011403.

(218). Zhang J; Yan S; Yuan D; Zhao Q; Tan SH; Nguyen N-T; Li W, A Novel Viscoelastic-Based Ferrofluid for Continuous Sheathless Microfluidic Separation of Nonmagnetic Microparticles. Lab Chip 2016, 16 (20), 3947–3956. 10.1039/C6LC01007E. [PubMed: 27722618]

(219). Lu X; DuBose J; Joo SW; Qian S; Xuan X, Viscoelastic Effects on Electrokinetic Particle Focusing in a Constricted Microchannel. Biomicrofluidics 2015, 9 (1), 014108. 10.1063/1.4906798. [PubMed: 25713690]

(220). Shim S; Stemke-Hale K; Noshari J; Becker FF; Gascoyne PRC, Dielectrophoresis Has Broad Applicability to Marker-Free Isolation of Tumor Cells from Blood by Microfluidic Systems. Biomicrofluidics 2013, 7 (1), 011808. 10.1063/1.4774307.

(221). Park S; Zhang Y; Wang T-H; Yang S, Continuous Dielectrophoretic Bacterial Separation and Concentration from Physiological Media of High Conductivity. Lab Chip 2011, 11 (17), 2893–2900. 10.1039/C1LC20307J. [PubMed: 21776517]

(222). Gupta V; Jafferji I; Garza M; Melnikova VO; Hasegawa DK; Pethig R; Davis DW, ApoStream™, a New Dielectrophoretic Device for Antibody Independent Isolation and Recovery of Viable Cancer Cells from Blood. Biomicrofluidics 2012, 6 (2), 024133. 10.1063/1.4731647.

(223). Beech JP; Jönsson P; Tegenfeldt JO, Tipping the Balance of Deterministic Lateral Displacement Devices Using Dielectrophoresis. Lab Chip 2009, 9 (18), 2698–2706. 10.1039/B823275J. [PubMed: 19704986]

(224). Calero V; Garcia-Sanchez P; Ramos A; Morgan H, Combining DC and AC Electric Fields with Deterministic Lateral Displacement for Micro and Nanoparticle Separation. Biomicrofluidics 2019, 13 (5), 054110. 10.1063/1.5124475. [PubMed: 31673301]

(225). Aghaamoo M; Aghilinejad A; Chen X; Xu J, On the Design of Deterministic Dielectrophoresis for Continuous Separation of Circulating Tumor Cells from Peripheral Blood Cells. Electrophoresis 2019, 40 (10), 1486–1493. 10.1002/elps.201800459. [PubMed: 30740752]

(226). Chang S; Cho Y-H, A Continuous Size-Dependent Particle Separator Using a Negative Dielectrophoretic Virtual Pillar Array. Lab Chip 2008, 8 (11), 1930–1936. 10.1039/B806614K. [PubMed: 18941695]

(227). White AM; Zhang Y; Shamul JG; Xu J; Kwizera EA; Jiang B; He X, Deep Learning-Enabled Label-Free On-Chip Detection and Selective Extraction of Cell Aggregate-laden Hydrogel Microcapsules. Small 2021, 10.1002/smll.202100491.

(228). Shamloo A; Yazdani A; Saghafifar F, Investigation of a Two-Step Device Implementing Magnetophoresis and Dielectrophoresis for Separation of Circulating Tumor Cells from Blood Cells. Eng. Life Sci 2020, 20 (7), 296–304. 10.1002/elsc.202000001. [PubMed: 32647508]

(229). Blaire G; Masse A; Zanini LF; Gaude V; Delshadi S; Honegger T; Peyrade D; Weidenhaupt M; Dumas-Bouchiat F; Bruckert F; Cugat O; Reyne G, Hybrid Bio-Mag-MEMS Combining Magnetophoresis and Dielectrophoresis. Eur. Phys. J. B 2013, 86 (4), 165. 10.1140/epjb/e2013-30679-1.

(230). Liu C; Lagae L; Borghs G, Manipulation of Magnetic Particles on Chip by Magnetophoretic Actuation and Dielectrophoretic Levitation. Appl. Phys. Lett 2007, 90 (18), 184109. 10.1063/1.2736278.

(231). Hunt TP; Westervelt RM, Dielectrophoresis Tweezers for Single Cell Manipulation. Biomed. Microdevices 2006, 8 (3), 227–230. 10.1007/s10544-006-8170-z. [PubMed: 16718407]

(232). Qiang Y; Liu J; Du E, Dynamic Fatigue Measurement of Human Erythrocytes Using Dielectrophoresis. Acta Biomater 2017, 57, 352–362. 10.1016/j.actbio.2017.05.037. [PubMed: 28526627]

(233). Barik A; Zhang Y; Grassi R; Nadappuram BP; Edel JB; Low T; Koester SJ; Oh S-H, Graphene-Edge Dielectrophoretic Tweezers for Trapping of Biomolecules. Nat. Commun 2017, 8 (1), 1867. 10.1038/s41467-017-01635-9. [PubMed: 29192277]

(234). Wu M; Ozcelik A; Rufo J; Wang Z; Fang R; Jun Huang T, Acoustofluidic Separation of Cells and Particles. Microsyst. Nanoeng 2019, 5 (1), 32. 10.1038/s41378-019-0064-3. [PubMed: 31231539]

(235). Ravula SK; Branch DW; James CD; Townsend RJ; Hill M; Kaduchak G; Ward M; Brener I, A Microfluidic System Combining Acoustic and Dielectrophoretic Particle Preconcentration and Focusing. Sens. Actuators, B 2008, 130 (2), 645–652. 10.1016/j.snb.2007.10.024.

(236). Wiklund M; Günther C; Lemor R; Jäger M; Fuhr G; Hertz HM, Ultrasonic Standing Wave Manipulation Technology Integrated Into a Dielectrophoretic Chip. Lab Chip 2006, 6 (12), 1537–1544. 10.1039/B612064B. [PubMed: 17203158]

(237). Ghayour R; Hojjat Y; Karafi MR; Sadeghiyan H, Development of a Hybrid DEP-SAW Device for Trapping/Sensing Target Cells. Appl. Acoust 2018, 141, 355–361. 10.1016/j.apacoust.2018.07.028.

(238). Smith AJ; O'Rorke RD; Kale A; Rimsa R; Tomlinson MJ; Kirkham J; Davies AG; Wälti C; Wood CD, Rapid Cell Separation with Minimal Manipulation for Autologous Cell Therapies. Sci. Rep 2017, 7 (1), 41872. 10.1038/srep41872. [PubMed: 28150746]

(239). Çetin B; Özer MB; Çağatay E; Büyükkoçak S, An Integrated Acoustic and Dielectrophoretic Particle Manipulation in a Microfluidic Device for Particle Wash and Separation Fabricated by Mechanical Machining. Biomicrofluidics 2016, 10 (1), 014112–014112. 10.1063/1.4940431. [PubMed: 26865905]

(240). Nge PN; Rogers CI; Woolley AT, Advances in Microfluidic Materials, Functions, Integration, and Applications. Chem. Rev 2013, 113 (4), 2550–2583. 10.1021/cr300337x. [PubMed: 23410114]

(241). Rivet C; Lee H; Hirsch A; Hamilton S; Lu H, Microfluidics for Medical Diagnostics and Biosensors. Chem. Eng. Sci 2011, 66 (7), 1490–1507. 10.1016/j.ces.2010.08.015.

(242). Hamada R; Suehiro J; Nakano M; Kikutani T; Konishi K Development of Rapid Oral Bacteria Detection Apparatus Based on Dielectrophoretic Impedance Measurement Method. IET Nanobiotechnol [Online], 2011, 5(2), 25–31. 10.1049/iet-nbt.2010.0011. [PubMed: 21495776]

(243). Di Trapani M; Manaresi N; Medoro G, DEPArray™ system: An Automatic Image-Based Sorter for Isolation of Pure Circulating Tumor Cells. Cytometry, Part A 2018, 93 (12), 1260–1266. 10.1002/cyto.a.23687.

(244). Henslee EA; Torcal Serrano RM; Labeed FH; Jabr RI; Fry CH; Hughes MP; Hoettges KF, Accurate Quantification of Apoptosis Progression and Toxicity Using a Dielectrophoretic Approach. Analyst 2016, 141 (23), 6408–6415. 10.1039/C6AN01596D. [PubMed: 27774532]

(245). Mahabadi S; Labeed FH; Hughes MP, Effects of Cell Detachment Methods on the Dielectric Properties of Adherent and Suspension Cells. Electrophoresis 2015, 36 (13), 1493–1498. 10.1002/elps.201500022. [PubMed: 25884244]

(246). Balasubramanian P; Kinders RJ; Kummar S; Gupta V; Hasegawa D; Menachery A; Lawrence SM; Wang L; Ferry-Galow K; Davis D; Parchment RE; Tomaszewski JE; Doroshow JH, Antibody-Independent Capture of Circulating Tumor Cells of Non-Epithelial Origin with the Apostream® System. PLoS One 2017, 12 (4), e0175414. 10.1371/journal.pone.0175414. [PubMed: 28403214]

(247). Kumar RTK; Kanchustambham P; Kinnamon D; Prasad S, 2D Dielectrophoretic Signature of Coscinodiscus Wailesii Algae in Non-Uniform Electric Fields. Algal Res 2017, 27, 109–114. 10.1016/j.algal.2017.08.031.

(248). Zhu JJ; Tzeng TRJ; Xuan XC, Continuous Dielectrophoretic Separation of Particles in a Spiral Microchannel. Electrophoresis 2010, 31 (8), 1382–1388. 10.1002/elps.200900736. [PubMed: 20301126]

(249). Zhu JJ; Xuan XC, Particle Electrophoresis and Dielectrophoresis an Curved Microchannels. J. Colloid Interf. Sci 2009, 340 (2), 285–290. 10.1016/j.jcis.2009.08.031.

(250). Li M; Li SB; Li WH; Wen WJ; Alici G, Continuous Manipulation and Separation of Particles Using Combined Obstacle and Curvature-Induced Direct Current Dielectrophoresis. Electrophoresis 2013, 34 (7), 952–960. 10.1002/Elps.201200546. [PubMed: 23436345]

(251). Zhang LJ; Bastemeijer J; Mollinger J; Bossche A In Continuous Dielectrophoretic Separation in the Iterative Curves Using DC-Biased AC Electric Fields, The 3rd IEEE Int. Conf. on Nano/Micro Eng. Mol. Syst., Sanya, China, 2008. DOI: 10.1109/NEMS.2008.4484460

(252). Zhang L; Bastemeijer J; Mollinger JR; Bossche A, Fabrication and Experimental Verification of a Dielectrophoretic Separation Device. Proc. 2009 IEEEE Sens. Conf, 2009, 1–3, 1168–1171. 10.1109/ICSENS.2009.5398585

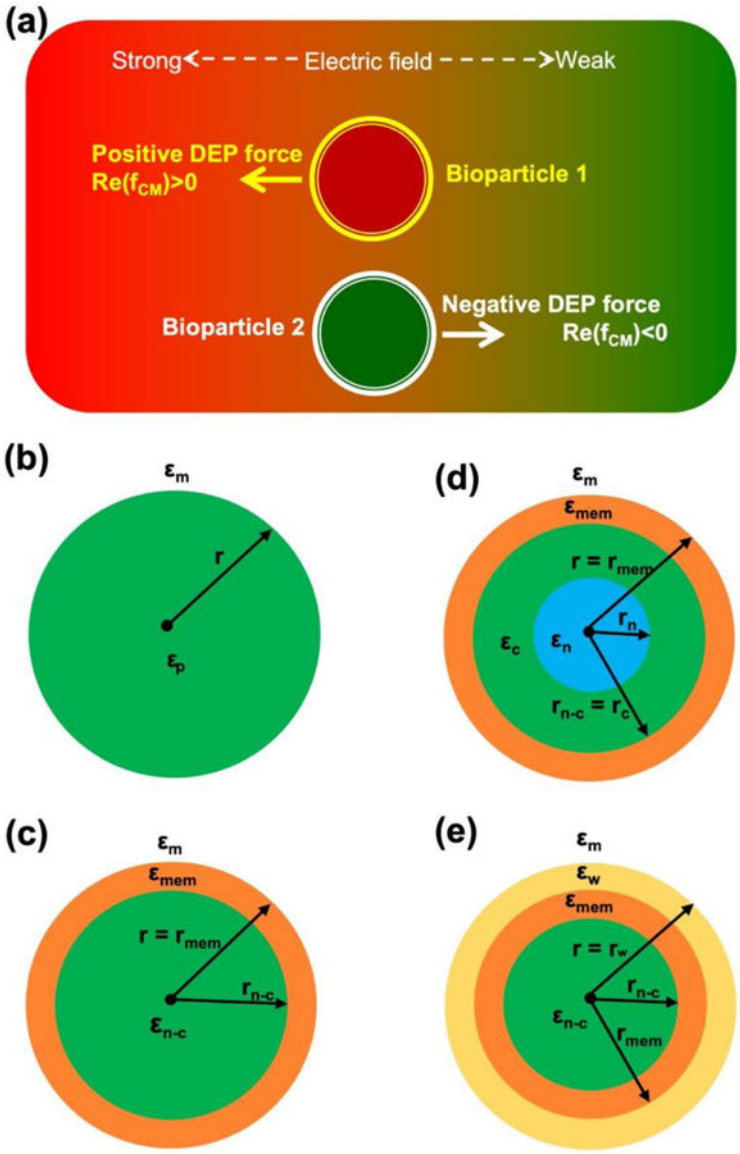

Fig. 1.

DEP responses and models used for DEP analysis of bioparticles. (a) Positive versus negative DEP forces. (b) Single-layer model. (c) Two-layer model. (d) Three-layer model for mammalian cells without a cell wall. (e) Three-layer model for plant cells with a cell wall.

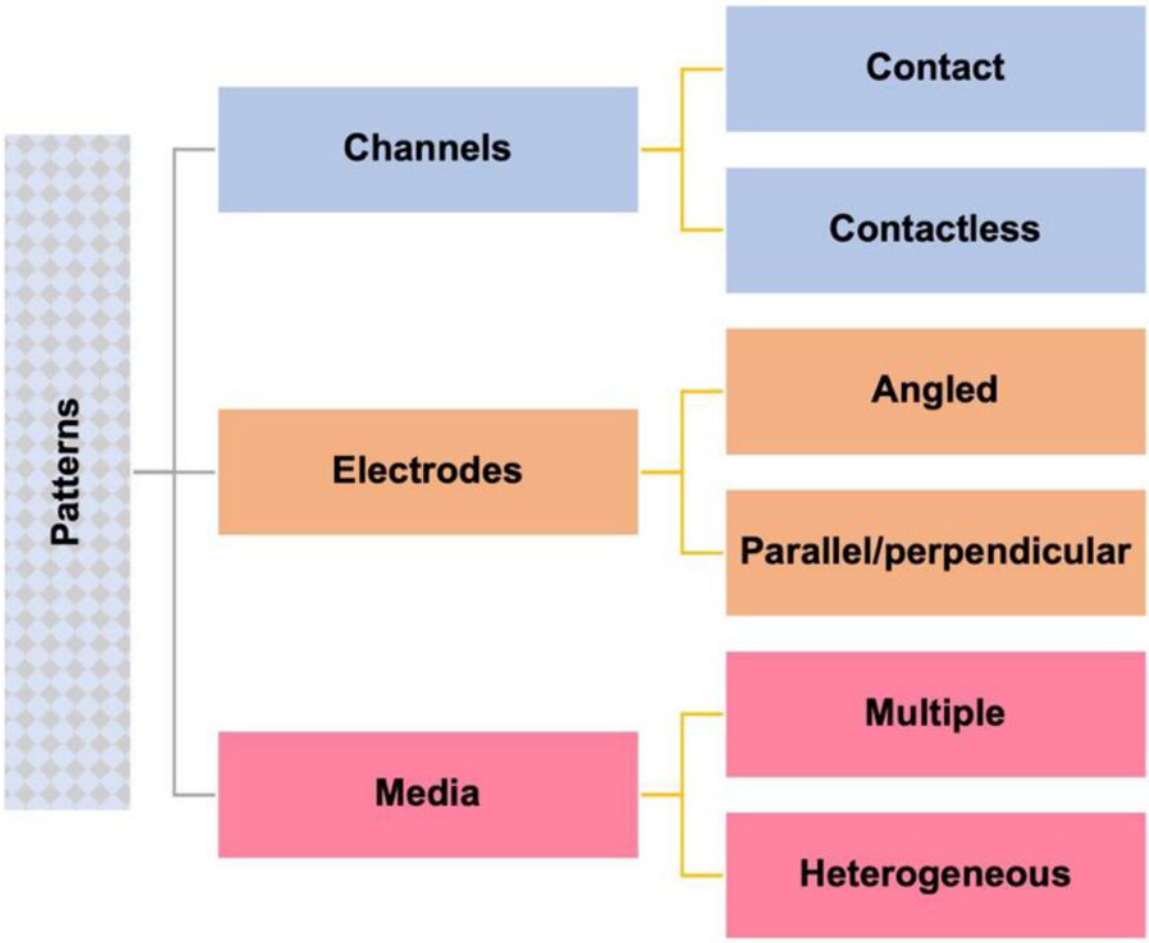

Fig. 2.
Categorization of DEP devices based on their patterns of channels, electrodes, and media for generating electric field gradient.

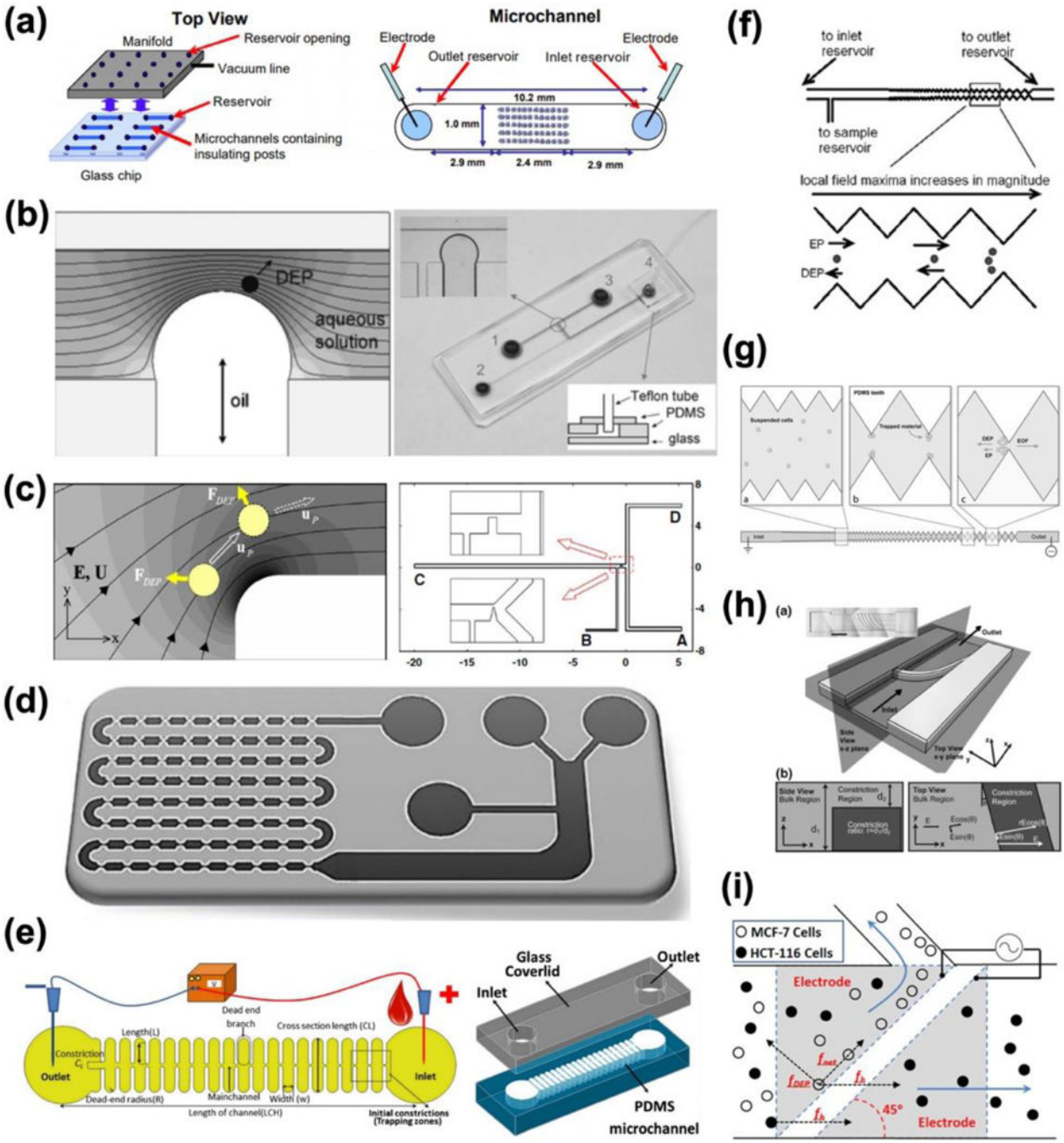

Fig. 3.

Some typical channel patterns of contact DEP devices. The devices have (a) insulating posts to separate various cells and particles, (b) an oil droplet to sort polystyrene particles based on their size, (c) a rectangular or a triangular block to sort fixed white blood cells and breast cancer cells individually based on their size, (d) a microfluidic channel with multiple rows uses an array of localized electric fields for DEP separation of breast cancer cells spiked in whole blood, (e) a corrugated microchannel for hydrodynamic trapping of RBCs, (f) a sawtooth structure to separate live and dead bacteria, (g) a sawtooth insulator-based channel

for separation of Escherichia coli bacteria based on their electrokinetic properties and (h) an angled structure to separate microparticles based on their size. i) a cell sorter with optically transparent electrodes that separates cancer cells based on their cross-over frequencies. (a) Reproduced with permission from ref. [87]. Copyright 2004 American Chemical Society. (b) Reproduced with permission from ref. [123]. Copyright 2014 Royal Society of Chemistry. (c) Reproduced with permission from ref. [120]. Copyright 2007 Springer Nature. (d) Reproduced with permission from ref. [128]. Copyright 2021 John Wiley and Sons. (e) Reproduced with permission from ref. [129]. Copyright 2015 Springer Nature. (f) Reproduced with permission from ref. [86]. Copyright 2007 American Chemical Society. (g) Reproduced with permission from ref. [121]. Copyright 2011 Springer Nature. (h) Reproduced with permission from ref. [74]. Copyright 2007 American Chemical Society. (i) Reproduced with permission from ref. [141]. Copyright 2013 American Institute of Physics.

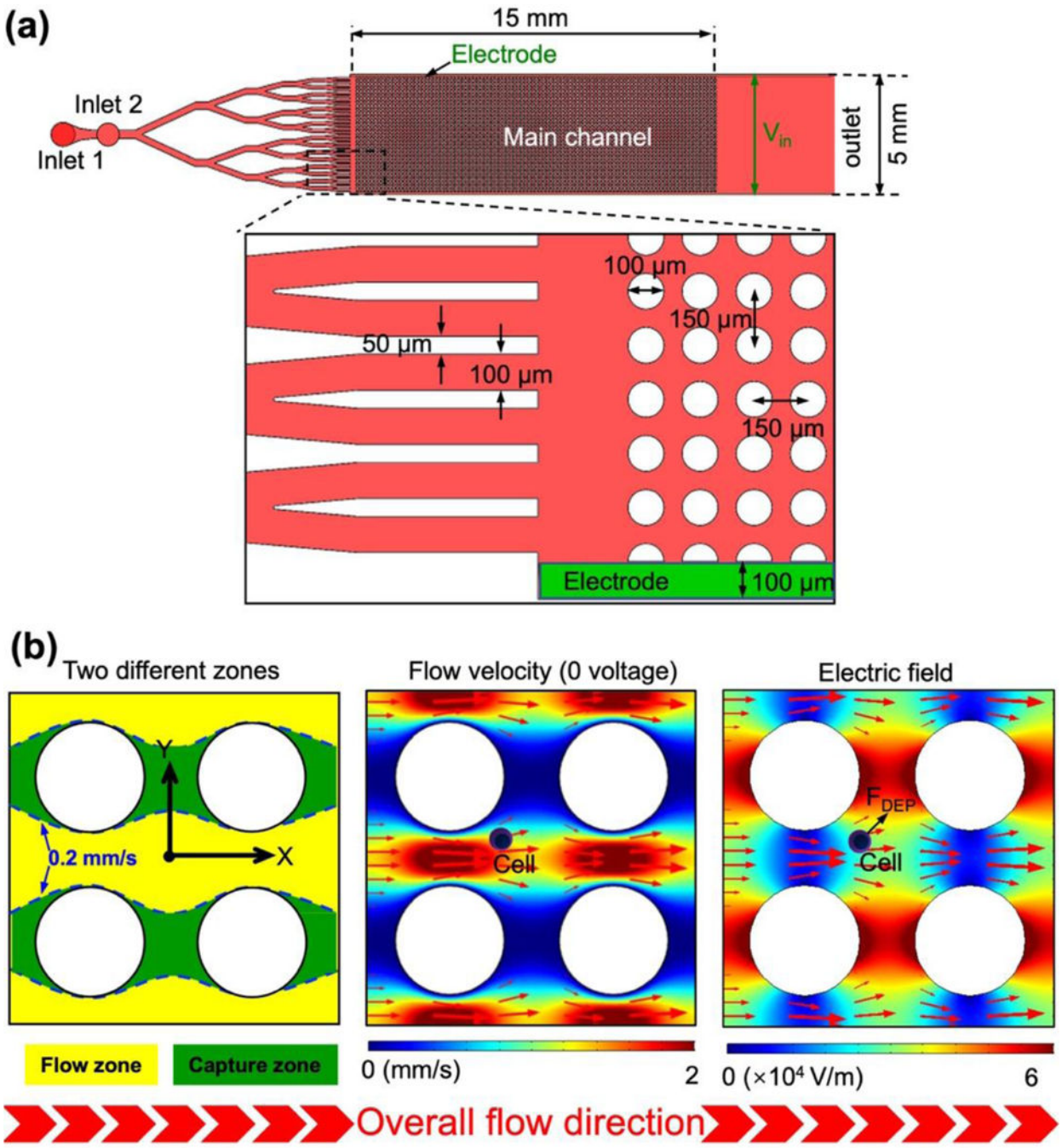

Fig. 4.

Channel pattern of the ZonesChip device. (a) Device pattern overview and dimensions. Two parallel electrodes were used to apply an electric field, and the electric field gradient was generated by the patterned microposts in the main channel. (b) Diagram of flow and capture zones (left), flow velocity (middle), and electric field strength (right). The main channel was separated into a capture zone with high electric field intensity and low flow speed, and a flow zone with low electric field intensity and high flow speed. Cells moving in the main

channel can be moved into the capture zone from the flow zone by DEP force. (a and b) Reproduced with permission from ref. [71]. Copyright 2019 Elsevier.

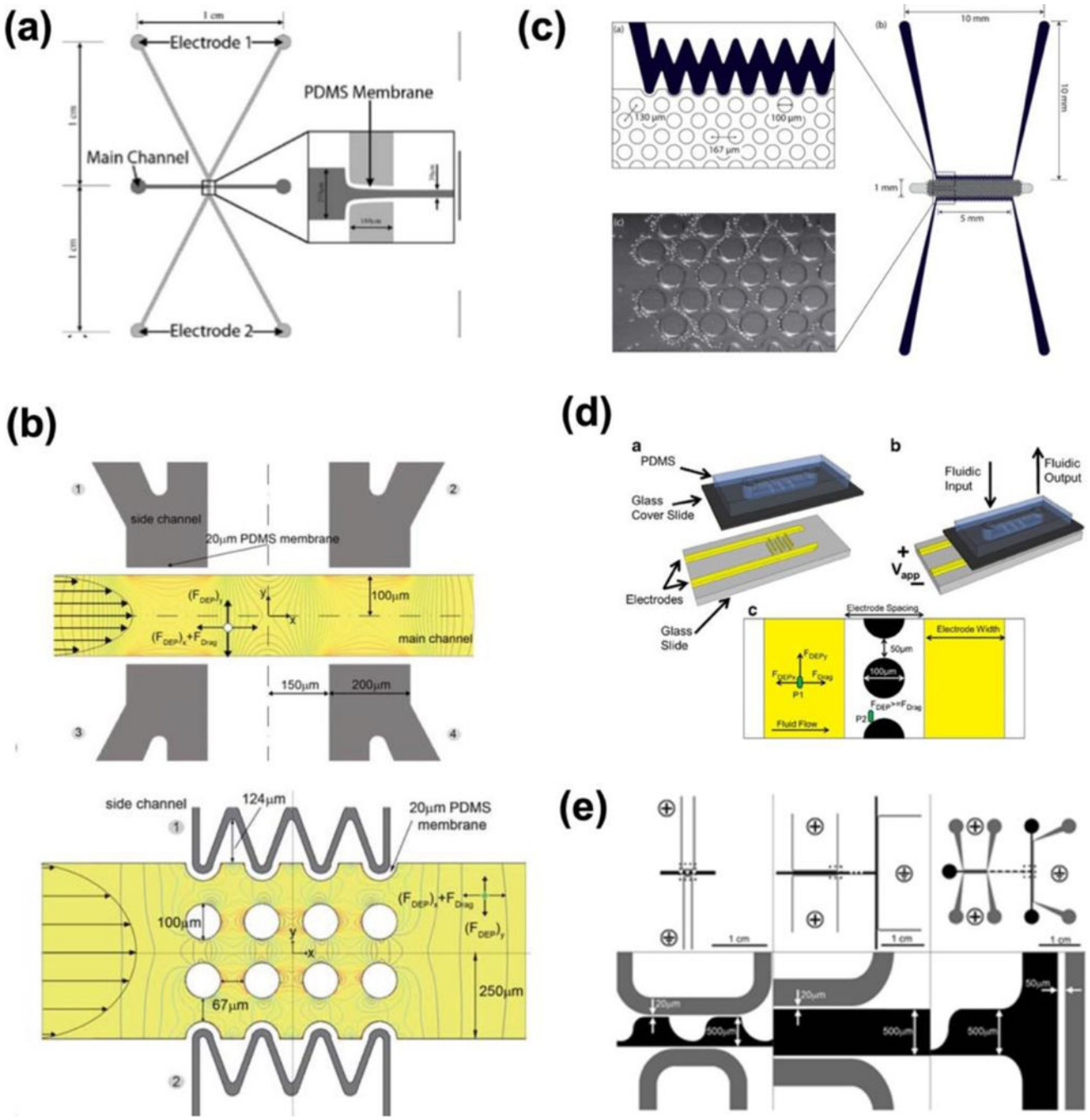

Fig. 5.

Some typical channel patterns of contactless DEP devices. The devices with channel patters (a) that allow for three cell lines, THP-1 human Leukemia monocytes, MCF-7 breast cancer cells, and MCF-10A breast cells, to be distinguished through their unique responses to DEP, (b) for separating live and dead THP-1 human leukemia monocytes, (c) for separating prostate tumor-initiating cells from regular tumor cells, (d) that use both an AC and a DC electric fields to drive and trap polystyrene microspheres, (e) for separating Escherichia coli cells from polystyrene beads. (a) Reproduced with permission from ref. [142]. Copyright

2009 Springer Nature. (b) Reproduced with permission from ref. [56]. Copyright 2010 Royal Society of Chemistry. (c) Reproduced with permission from ref. [57]. Copyright 2011 Royal Society of Chemistry. (d) Reproduced with permission from ref. [143]. Copyright 2013 Springer Nature. (e) Reproduced with permission from ref. [144]. Copyright 2011 Elsevier.

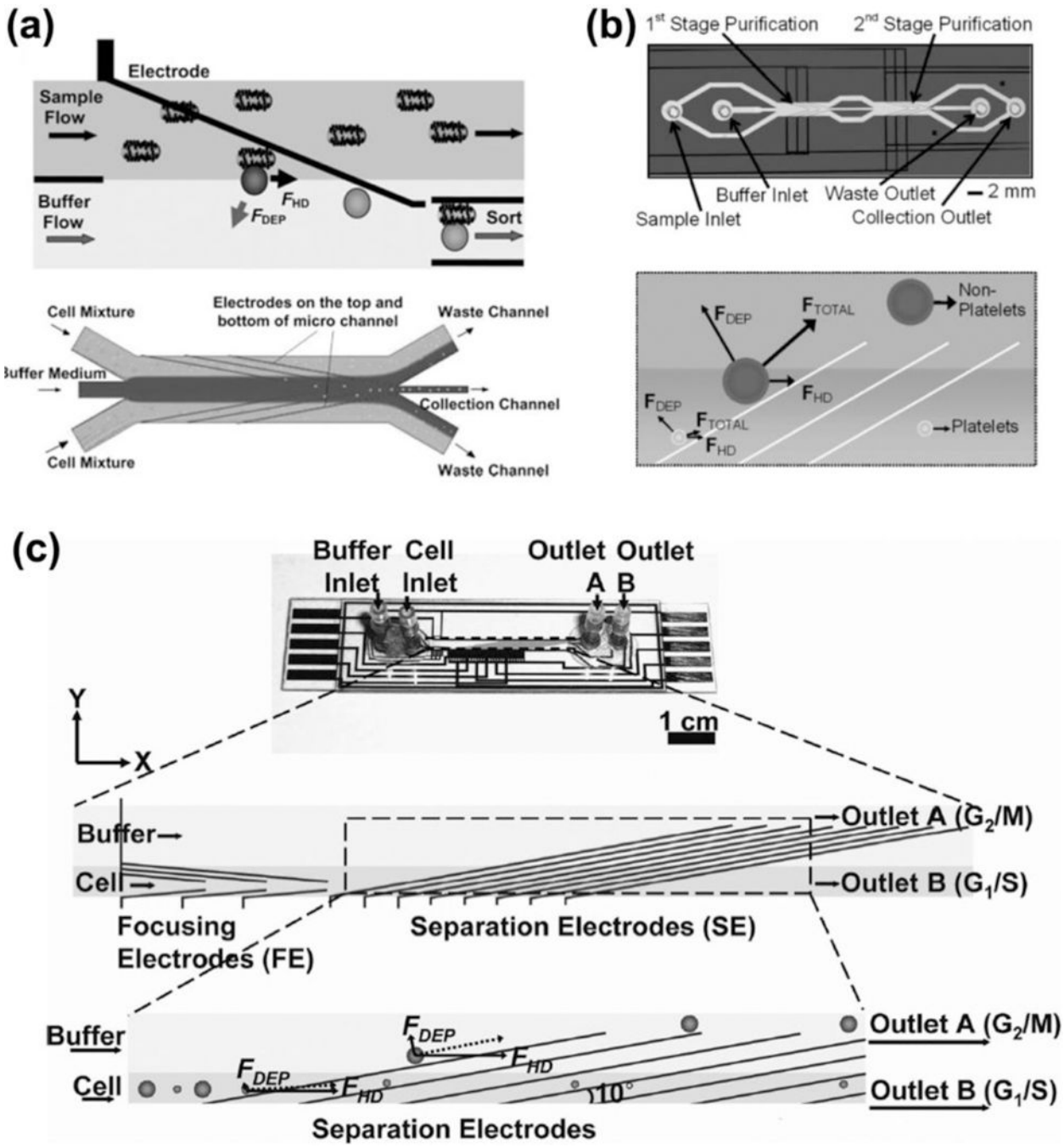

Fig. 6.

Angled electrode patterns. DEP devices with angled electrodes (a) for separation of rare target E. coli cells labeled with streptavidin-coated polystyrene beads, and nontarget E. coli cells, (b) for separation of platelets from diluted whole blood, and (c) for separation of polystyrene beads based on their size, and human breast ductal carcinoma cells in different cell-cycle phases. (a) Reproduced with permission from ref. [154]. Copyright 2005 The National Academy of Sciences. (b) Reproduced with permission from ref. [155]. Copyright

2008 John Wiley and Sons. (c) Reproduced with permission from ref. [156]. Copyright 2007 The National Academy of Sciences of the USA.

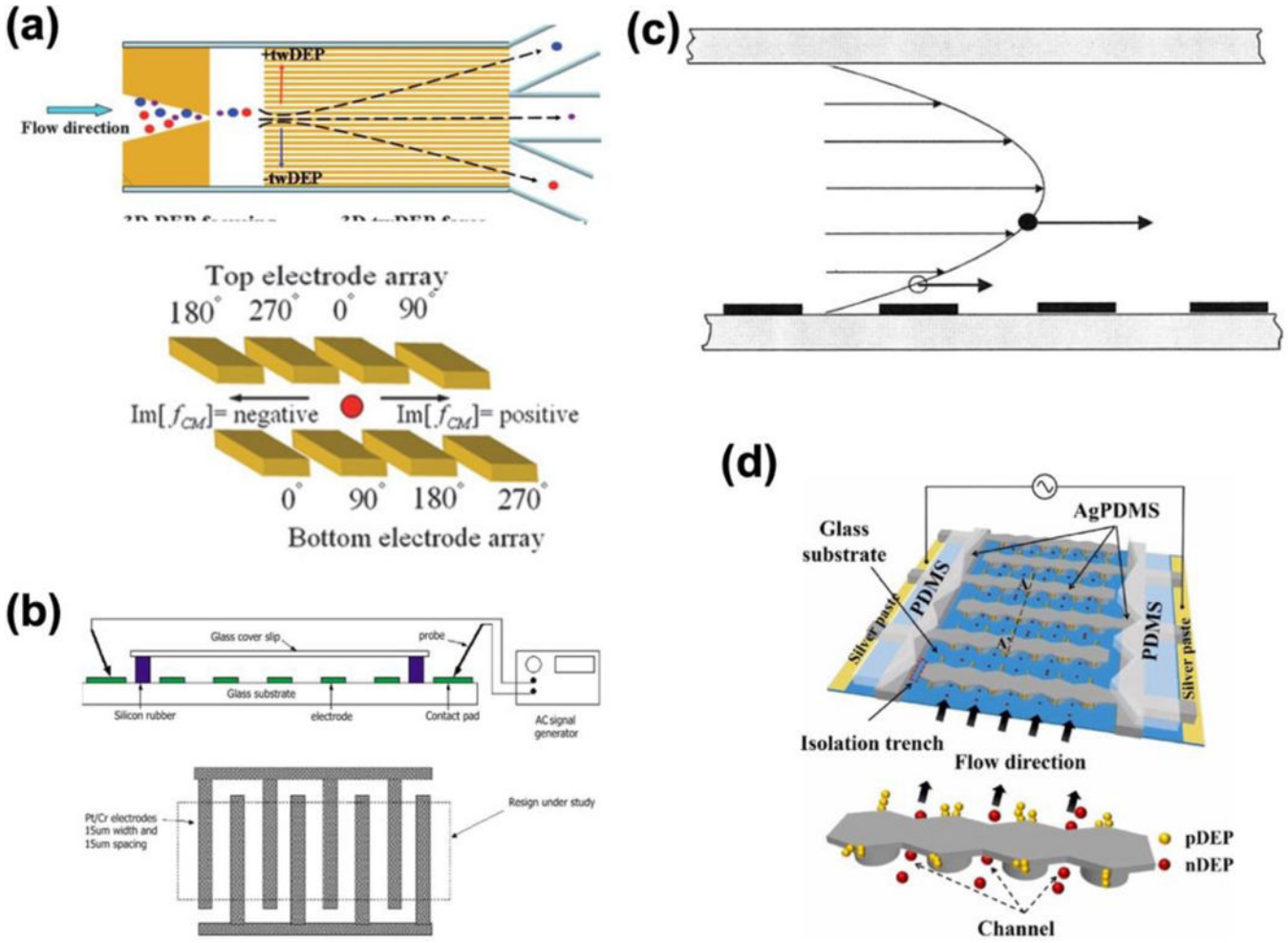

Fig. 7.

Parallel/perpendicular electrode patterns. DEP device with parallel/perpendicular electrodes (a) for separation of red blood cells from debris-filled heterogeneous samples and poly-dispersed liposomes based on their size using changing-phase DEP, (b) for separation of live and dead Listeria innocua cells using constant-phase DEP, (c) for separation of erythrocytes and latex beads using constant-phase DEP, and (d) for separation of human erythrocyte cells from similar-size polymer beads using constant-phase DEP. (a) Reproduced with permission from ref. [172]. Copyright 2001 Royal Society of Chemistry. (b) Reproduced with permission from ref. [173]. Copyright 2008 John Wiley and Sons. (c) Reproduced with permission from ref. [174]. Copyright 1998 Elsevier. (d) Reproduced, with permission, from ref. [178]. Copyright 2019 IEEE.

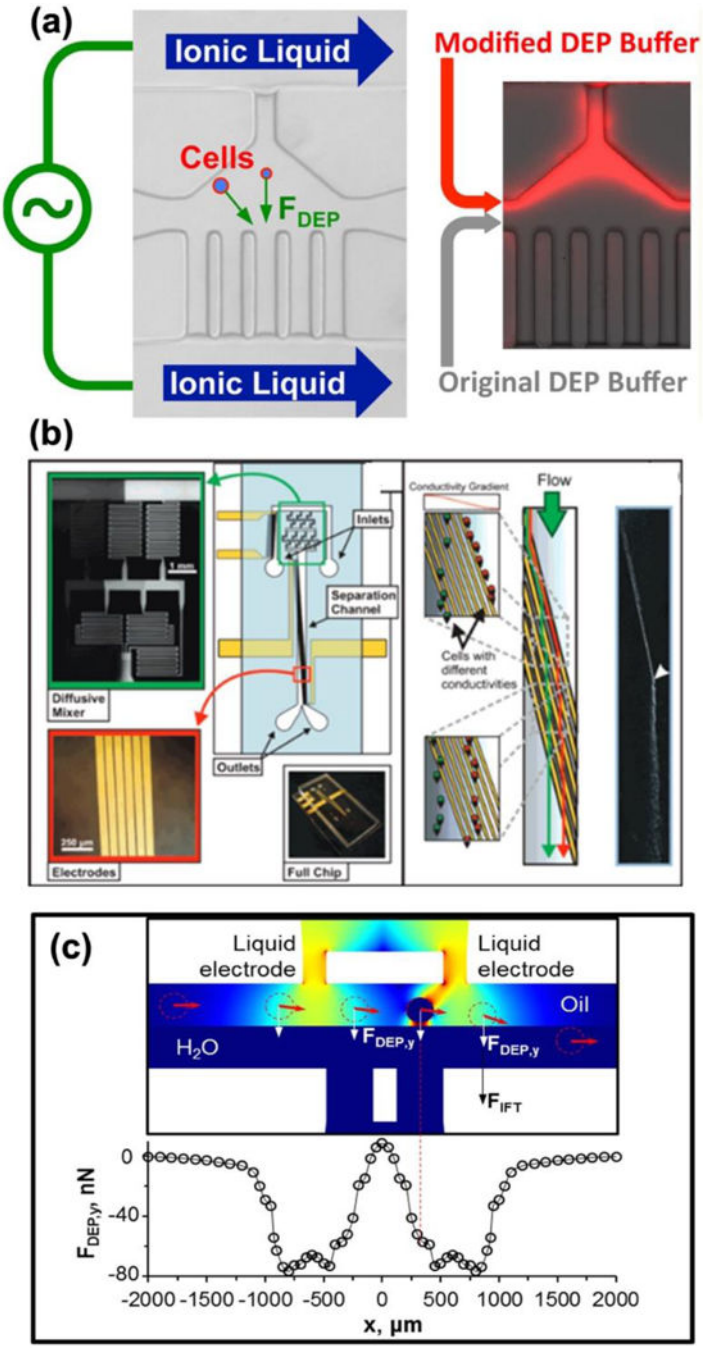

Fig. 8.

Media patterns. DEP devices with (a) two kinds of DEP buffers of different electrical conductivities to separate several types of cells, (b) DEP media of various conductivities to sort polystyrene beads based on size, and live versus dead budding yeast Saccharomyces cerevisiae, and (c) oil emulsion and aqueous solution of very different electrical conductivities to extract hydrogel microcapsules from the oil emulsion into aqueous solution. (a) Reproduced with permission from ref. [127]. Copyright 2016 American Chemical Society. (b) Reproduced with permission from ref. [21]. Copyright 2008 American

Chemical Society. (c) Reproduced with permission from ref. [53]. Copyright 2015 John Wiley and Sons

Table 1.

A summary of different models used for modeling different bioparticles. NA: Not available

Study	Cell	Bioparticle radius	Conductivity of the medium
Single-layer model			
Srivastava[70] Han[100]	Erythrocyte	2–4 μm 2.6 μm	NA 17 mS/m
Huang[97] LaLonde[98]	Yeast	4 μm 3.15 μm	10 mS/m 20 mS/m
Madiyar[99]	Vaccinia virus	125 nm	NA
Siebman[101] Gallo-Villanueva[102]	Algae		2.25 S/m 1.87 S/m
Two-layer model			
Becker[112]	Leukemia cells	5 μm	56 mS/m
Su[107]	HL-60 cells	6.1 μm	1.36 S/m
Huang[95]	Fission yeast cells	NA	NA
Ibsen[107]	Exosomes	25–75 nm	NA
Chan[106]	Liposomes	≥1.25 μm	13 mS/m
Three-layer model for mammalian cells without a cell wall			
Hao-Wei[107]	HL-60 cells	6.1 μm	0.89 S/m
Becker[112]	Leukemia cells	5 μm	56 mS/m
Irimajiri[110]	lymphoma cell	6.5 μm	10 mS/cm
Nguyen[114]	CTCs RBCs	5 μm 3.25 μm	55 mS/m
Three-layer model for plant cells with a cell wall			
Roberto[102]	Plant protoplasts	NA	NA
Aldeaeus[116]	Bacteria	5 μm	0.23 S/m
Kumar[247]	Algae	10 μm	~47 mS/cm

Table 2.

A summary of the media commonly used for bioparticle manipulation in DEP devices with the three different methods of DEP generation. NA: Not available

Study	DEP medium	Conductivity of the medium	Bioparticle studied
Patterns of channels			
Lapizco-Encinas[87, 118–119]	Deionized water	2.25 mS/m	Bacterial cells (Live and dead E. coli)
	Deionized water with NaOH and KCl	2.2 and 10.4 mS/m	
Barbulovic-Nad[123]	Deionized water	NA	-Polystyrene particles
Kang[120]	Lysis buffer (1× DMEM)	NA	White blood cells and mammalian breast cancer cells
	Nutrition solutions:10 mM Tris, 50 mM NaCl, 250 mM Trehalose, and 0.02% EDTA	NA	
Srivastava[124]	Isotonic buffers: dextrose and PBS at pH 7.0	0.52 to 9.1 mS/cm	Erythrocyte
Zhu[248–249]	1 mM phosphate buffer with Tween 20 (0.5% v/v)	20 mS/m	Polystyrene particles
	10 mM phosphate buffer with Tween 20 (0.5% v/v)	200 mS/m	
Pysher[86]	1 mM phosphate buffer	NA	Bacterial cells (Bacillus subtilis, E. coli, and Staphylococcus epidermidis)
Hawkins[74]	Deionized water	NA	Polystyrene spheres
Li[250]	10 mM NaCl solution	NA	10–15 μm polystyrene beads comparable to white blood cells
Sun[127]	DEP buffer: 10% (w/v) sucrose and 0.3% (w/v) glucose	1 mS/m	-Live and dead PC-3 cells
Shafiee[56]	DEP buffer: 8.5% (w/v) sucrose, 0.3% (w/v) glucose, and 0.725%(v/v) RPMI	10 mS/m	THP-1 human leukemia monocytes
Salmanzadeh[57]	DEP buffer: 8.5% (w/v) sucrose, 0.3% (w/v) glucose, and 0.725%(v/v) RPMI	11 mS/m	prostate tumor initiating cells
Zellner[143]	Deionized water	0.8 mS/m	E. coli strain MG1655
Sano[144]	DEP buffer: 8.5% (w/v) sucrose, 0.3% (w/v) glucose, and 0.725%(v/v) RPMI	11 mS/m	THP-1 human leukemia monocytes and red blood cells
Patterns of electrodes			
Kang[147]	0.75 mM sodium borate buffer	27 mS/m	Yeast cells and polystyrene particles
Hu[154]	0.1×PBS, 1% BSA, and 20%(v/v) glycerol	NA	Bacterial cells (E. coli)
Pommer[155]	LEC buffer: sugar-based solution	50 mS/m	Platelets
Kim[156]	0.1×PBS, 1% BSA and 20% (v/v) glycerol	100 and 200 mS/m	MDA-MB-231 human breast tumor cells
	0.1×PBS, 2% BSA, 1mM EDTA, and 8.5% (v/v) sucrose	100 to 200 mS/m	
Cheng[172]	280 mM D-mannitol solution and 1× PBS solution in an 11:1 ratio	120 mS/m	Erythrocytes and Staphylococcus aureus
Li[173]	Deionized water	0.2 mS/m	Listeria innocua cells
Rousselet[174]	2.5% mannitol solution with NaCl	1, 2, 5, and 10 mS/m	Erythrocytes and latex beads
Lewpiriyawong[148]	NaCl solution	38 and 60 mS/m	Yeast cells) and E. coli

Study	DEP medium	Conductivity of the medium	Bioparticle studied
Zhang[251–252]	Deionized water	NA	Polystyrene beads
Patterns of media			
Sun[127]	Original DEP buffer: 10% (w/v) sucrose and 0.3% (w/v) glucose, and modified DEP buffer: 10% (w/v) sucrose, 0.3% (w/v) glucose, and 0.8% (v/v) PBS	1 and 14 mS/m	-Live and dead PC-3 cells
Vahey[21]	Deionized water, 1% BSA, and PBS	10.5, 19, 33, 40, and 55 mS/m	Yeast cells
Huang[53] Sun[54] White[227]	Oil emulsion	~0 mS/m	C3H10T1/2 cells MCF-7 cell aggregate MCF-7 cell aggregate